Version of Record: https://www.sciencedirect.com/science/article/pii/S0022169418307996
Manuscript_048bf39b4a2de76bac58b8113a46259d

Simple and Modular Integrated Modeling of Storm Drain Network with Gridded Distributed Hydrologic Model via Grid-Rendering of Storm Drains for Large Urban Areas

by

Hamideh Habibi[*,1], Dong-Jun Seo

Department of Civil Engineering, The University of Texas at Arlington, Arlington, TX, USA

Submitted to the Journal of Hydrology

September 3, 2018

---

[1]Now at Prairie View A&M University, Prairie View, TX, USA

[*]Corresponding Author: Hamideh Habibi, College of Agriculture and Human Sciences, Cooperative Agricultural Research Center, Prairie View A&M University, P.O. Box 519, Prairie View, TX 77446-0519

Email: hamideh.habibi@mavs.uta.edu, Phone: 936-261-5042

© 2018 published by Elsevier. This manuscript is made available under the Elsevier user license
https://www.elsevier.com/open-access/userlicense/1.0/

Abstract

For accurate flash flood forecasting and effective stormwater planning and management in urban areas, it is necessary to model not only the natural channel systems but also the large and complex networks of storm drains. In this work, we describe a modular storm drain model that can easily be coupled with existing gridded distributed hydrologic models for real-time flash flood forecasting, and stormwater planning and management for large urban areas (> 100 km^2). A salient feature of our approach is the use of the equivalent storm drain network (ESDN) which approximates the actual network on the same grid as that of the distributed hydrologic model, thereby rendering coupling simple and modular. In the integrated model, storm-drain flow occurs through the simplified network coarsened to the resolution of the distributed hydrologic model without full 1D-2D dynamics or very detailed man-made structures and features modeled. The integrated model is applied to a 144.6 km^2 area of five urban catchments in the Cities of Arlington and Grand Prairie in Texas, US. Comparisons at selected locations using kinematic-wave flow simulations show that the ESDN approximates the flow through the original network very well with attendant savings in computational amount and reduction in modeling complexities. The impact of the storm drain network is assessed via a combination of simulation experiments, sensitivity analysis and limited comparison with observed flow. It is shown that the storm drain network in highly urbanized catchments in the study area is very effective in reducing surface flow at most locations for about 30 min following onset of significant rainfall, that the existing stormwater infrastructure would lose effectiveness for approximately 30% of the study area with a 15% increase in imperviousness relative to the current conditions, and that significant uncertainties exist in partitioning of surface flow into storm drain and natural channel flows due to sensitivity to inlet flow modeling. With greatly reduced computing cost and

modeling complexity, the proposed approach offers a practical solution for integrated stormwater modeling for large urban areas for a wide range of applications. The proposed approach cannot, however, resolve flow at sub-grid scales and hence is not appropriate for very detailed modeling for small areas.

Keywords: equivalent storm drain network, distributed hydrologic modeling, integrated modeling, flash flood forecasting, stormwater planning and management.

1 Introduction

Flooding is one of the most significant natural hazards in urban areas and a significant cause for economic loss and inconvenience to the residents. To mitigate hazards and to reduce negative impacts of flooding, urban municipalities operate storm drain networks of varying capacity and complexity. Whereas the conveyance capacities of storm drain systems are generally much smaller than those of the natural channel systems (Rafieeinasab et al. 2015), storm drain networks may significantly alter the severity of flooding and other negative impacts depending on the location of flooding and the magnitude of rainfall. For accurate flash flood forecasting in urban areas, it is therefore necessary to model not only the natural channel systems but also the large and complex networks of storm drains (Hénonin et al. 2010). Such a capability is also important for planning and management of stormwater infrastructure which has traditionally been designed on a site-by-site basis with the goal of keeping the post-development peak flow from flooding events the same as before. Such practice, however, does not reduce the runoff or the total volume of stormwater and may still produce flooding downstream. Also, with site-by-site design, it is not possible to fully account for spatiotemporal variations of runoff and flow through natural and man-made hydrologic and hydraulic systems or spatiotemporal variability of precipitation beyond the site scale. As such, the resulting stormwater system may not work effectively at larger watershed scales. Indeed, McCuen (1979) and Emerson et al. (2005) showed that an unplanned system of site-based stormwater control measures or best management practices can actually increase flooding on a watershed scale owing to the effect of many facilities discharging into a receiving water body in an uncoordinated fashion - causing the very flooding problem the individual basins were built to solve (NRC 2008).

The ability to model the natural channel and storm drain systems jointly for large urban areas also allows objective assessment of performance of stormwater infrastructure from heavy-to-extreme precipitation under changing conditions. Many researchers have assessed the impacts of climate change on urban drainage systems and analyzed specific impacts on different small urban areas (e.g., Watt et al. 2003; Mailhot et al. 2006a; Guo 2006; Denault et al. 2006; Arnbjerg-Nielsen et al. 2013). Increase in intensity and frequency of heavy-to-extreme rainfall events may cause increase in sewer overflows and urban flooding (Mailhot et al. 2006; Willems et al. 2012; Nazari et al. 2016). While the results vary depending on the urban catchment's response to such rainfall, most conclude that urban areas are subject to increased probability of surcharge and resulting flooding. As such, a critical need exists in stormwater planning and management for capability to assess the performance of large storm drain networks under heavy-to-extreme rainfall, changing land cover conditions and climate change (Norouzi et al. 2018).

Integrated modeling of flow through natural channels and storm drains for small urban areas is not new (Bonnifait et al. 2009; Kim et al. 2012; Neal et al. 2012; Schumann et al. 2013; Nguyen et al. 2015,Guidolin et al. 2012, Gires et al. 2015, Simões et al. 2011). Approaches such as 1D storm drain-2D surface flow modeling (Leandro et al. 2009) have gained wide popularity and acceptance in recent years. Many urban hydraulic models of varying levels of sophistication currently exist, such as HEC-1 (USACE 1985), TR-20 and TR-55 (SCS 1983, 1986), MOUSE (DHI 1995), InfoWorks ICM (Integrated Catchment Modeling, Innovyze 2012), MIKE URBAN (Andersen et al., 2004), and Stormwater Management Model (SWMM) (EPA 1971, Huber and Dickinson 1988), just to name a few. For real-time applications over large areas (> 100 km^2), however, such approaches quickly become impractical because of modeling complexities and extremely large computational requirements (Pina et al. 2016, Chen et al. 2012, Duncan et al. 2011, Leitão et al. 2010). Distributed hydrologic models (Reed et al. 2004, Smith et al. 2004), on the other hand, are more suitable for real-time application over large areas (Koren et al. 2004, Gochis et al. 2014) but are intended to simulate mainly surface flows. In order to add ability to model storm drains to distributed hydrologic models, an integration with hydraulic models is needed.

The objective of this work is to develop a storm drain model that can easily be integrated with the existing gridded distributed hydrologic models for real-time simulation of flow through both natural channels and storm drains for large urban areas. The specific research questions addressed are: 1) How to reduce the geometric complexity of a storm drain network into a simpler “equivalent” network?; 2) How to partition storm runoff into pipe and overland flow? What are the largest sources of uncertainty in the above partitioning?; 3) How does the storm drain network alter the hydrologic response of urban catchments? How does the response vary according to the size of the contributing area, land cover and rainfall magnitude?; and 4) What is the relative importance of natural channels and storm drains in stormwater management and flood control at different spatiotemporal scales? The new and significant contributions of this research are: 1) development of an integrated model capable of simulating flow through both natural channels and storm drains for real-time application for large urban areas; 2) development of an automatic algorithm for derivation of equivalent storm drain network (ESDN) for direct coupling with existing gridded distributed hydrologic model; and 3) advances in understanding of hydrologic response of urban catchments to heavy-to-extreme rainfall from site to catchment scales.

The rest of this paper is organized as follows. Section 2 describes the approach and method for integrated modeling. Section 3 describes the study area and data used. Section 4 presents the results. Section 5 summarizes the conclusions and future research recommendations.

2 Integrated modeling of natural channels and storm drain networks

The general approach adopted in this work is to develop a storm drain module that can be coupled with the existing gridded distribute models with minimum changes to the latter. The gridded distributed hydrologic model used in this work is the U.S. National Weather Service's (NWS) Hydrology Laboratory Research Distributed Hydrologic Model (RDHM) (Koren et al. 2004, NWS 2009). The RDHM has been used in many research and operational applications (Moreda et al. 2006; Reed et al. 2007; Nguyen et al. 2012; Fares et al. 2014; Habibi et al. 2016) and is recognized as one of the best performing distributed hydrologic models (Reed et al. 2004; Smith et al. 2012; Moreda et al. 2006). The RDHM operates on the rectangular Hydrologic Rainfall Analysis Project (HRAP) projection grid (Greene and Hudlow 1982) which has a resolution of approximately 4 km×4 km in mid-latitudes. Whereas the a priori parameters are available for the continental US at 1 HRAP resolution only, the RDHM can operate at higher resolutions of 1/2, 1/4, 1/8, 1/16 HRAP, etc. In this work, the 1/16 HRAP resolution, or about 250 m, is used throughout. The RDHM uses the Sacramento model (SAC, Burnash et al. 1973) for rainfall-runoff modeling and the kinematic wave model (Chow et al. 1988, Koren et al. 2004) for hillslope and channel routing. Surface runoff is routed within each cell through conceptual hillslopes that drain into the conceptual channel running through the same grid cell. Subsurface runoff from the SAC is drained directly into the conceptual channel.

In developing the storm drain module, modularity, simplicity and computational efficiency are of great importance so that it may easily be integrated with the existing distributed models with gridded hillslope and channel routing. By operating the storm drain module on the same grid as the gridded hydrologic model, one only needs to partition runoff into natural channel and storm drain flows at each grid box, route the flows separately, and discharge the storm drain flow into the natural channel at outfall locations. In this way, adding the storm drain module to the gridded distributed model amounts only to adding a sink to the existing channel routing model if the grid box contains inlets, and a source if the grid box contains outfalls. Fig 1 shows the schematic of this approach in the context of the RDHM. The above modelling approach entails significant simplification of the relevant processes due, e.g., to the coarse resolution of 250 m employed. As such, the proposed approach is not appropriate for certain applications which may require very high-resolution modeling. The spatial scale of the modeling domain of interest in this work is 100 to 1,000 times larger than that in typical 1D-2D application (Gires et al. 2015, Simões et al. 2011).The proposed approach hence represents a set of modeling choices carefully selected from the array of elements in storm drain and distributed hydrologic modeling toward an operational viable solution for large urban areas.

With the ESDN approach, the storm drain modeling (SDM) takes the following steps: 1) Determine the model resolution; 2) Derive the ESDN from the actual storm drain network to the resolution of the RDHM; 3) Run the SAC to determine surface and subsurface runoff for all grid cells; 4) Partition the surface runoff between the ESDN and the natural channel network for all grid cells; 5) Route the storm drain flow through the ESDN using a pipe-flow approach and discharge into the natural channels at outfall-containing grid cells, 6) Route the natural channel flow through the natural channel network; and 7) Repeat Steps 3 through 6 for all time steps. The following describes the storm drain module and its integration with the RDHM (Steps 2 through 6) in detail.

2.1 Hillslope routing

The water depth over the conceptual hillslopes in each grid cell is modeled via kinematic wave routing (Koren et al. 2004):

$$\frac{\partial h}{\partial t} + L_h \frac{\partial q_{L_h}}{\partial x} = R_s \qquad (1)$$

$$q_{L_h} = \frac{1}{L_h}\frac{1}{n} h^{5/3} S^{1/2} = 2D\,\frac{1}{n} h^{5/3} s^{1/2} \qquad (2)$$

where h denotes the water depth on the hillslopes (m), R_s denotes the surface runoff rate (m/s), q_{L_h} denotes the total discharge per unit area from all hillslopes in the grid box (m/s), L_h denotes the hillslope length (m) given by the area of a grid cell (m^2) divided by the total width of the hillslopes over which surface flow occurs (m), *S* denotes the slope of the hillslopes (dimensionless), *n* denotes the hillslope Manning roughness coefficient ($s/m^{1/3}$), *D* denotes the drainage density (m^{-1}), a parameter for subdividing a cell into equally sized overland flow planes, and t denotes time (s). The drainage density, D, represents the reciprocal of the characteristic length scale of a hillslope within a cell and a constant value of 2.5 (km^{-1}) is assumed in this work. The identity of $1/L_h=2D$ in Eq.(2) stems from the assumed symmetry of the conceptual hillslopes draining into the natural channel that runs in the middle of the grid box. For further details of the model and estimating parameters, the reader is referred to Koren et al. (2004).

2.2 Channel routing

With the inclusion of storm drain flow, the RDHM routing model for natural channels (Koren et al. 2004) is modified to the following:

$$\frac{\partial A}{\partial t}+\frac{\partial Q}{\partial x}=\frac{(R_g+q_{L_h})f_c}{L_c}-\frac{Q_{inlet}}{L_c}+\frac{Q_{outfall}}{L_c} \quad (3)$$

$$Q=Q_s A^m \quad (4)$$

where A denotes the wetted cross section of the natural channel (m^2), Q denotes the flow though the natural channel (m^3/s), R_g denotes the subsurface runoff rate from SAC (m/s), q_{L_h} denotes the overland flow rate per unit area at the hillslope outlet (m/s) (see Eqs.(1) and (2)), f_c denotes the grid cell area (m^2), L_c denote the channel length within a grid cell (m), Q_{inlet} denotes the total flow into the storm drains within the grid box (m^3/s), $Q_{outfall}$ denotes the total flow through all outfalls within the grid box (m^3/s), m denotes the exponent parameter, Q_s denotes the specific discharge (m/s), and m denotes an exponent parameter. In Eq.(3), the total flow into the storm drain network through the inlets in the grid cell cannot exceed the total flow generated from the hillslope at that grid cell or the total flow generated from the pavement area of the grid cell, Q_{pvmt} (see Subsection 2.4), i.e., $Q_{inlet} \le \min\{q_{L_h} f_c, Q_{pvmt}\}$. The a priori parameter grids of Q_s and m are available from the NWS for the continental US (CONUS) based on the 30-m resolution National Elevation Dataset from the NHDPlus Version 2 (NHDPlusV2, David et al. 2011). The cell-to-cell connectivity is derived with the Cell-Outlet-Tracing-with-an-Area-Threshold algorithm (Reed, 2003). In this work, the routing model parameters and the channel connectivity are rederived at 1/16 HRAP resolution using the NWS-developed programs. With Eq.(3), storm drain modeling amounts to modeling time-varying Q_{inlet} and $Q_{outfall}$ at all grid boxes which is described below.

2.3 Equivalent storm drain network (ESDN)

The purpose of the ESDN is to represent the actual network with a hydraulically equivalent virtual network that has only a single virtual pipe in each grid box. In this way, one may couple the storm drain module to the gridded distributed model only by adding sink and source terms in the existing channel routing model as shown in Eq.(3). Deriving the ESDN amounts to coarsening the real storm drain network such that the former approximates the mass and momentum balance of the latter within acceptable accuracy. Pipe networks generally consist of series and parallel pipes. All such configurations may be combined and converted into a simple equivalent pipe (Jeppson 1974). Multiple approaches exist for modeling equivalent pipe systems of series and parallel pipes under steady state and full flow conditions (Anderson et al 1995; Larock et al 2000). Most approaches are based on adjusting the diameter, and length or roughness of the pipes while keeping the other properties unchanged. The resulting equivalent network produces the same pressure heads and head losses as the original network for all flow rates. The main limitation with the above simplification is that, although the resulting network is hydraulically equivalent to the original network, it does not preserve travel time due to the steady-state assumption. To approximate both the hydraulics and the travel time for series and parallel pipes, Raczynski et al. (2008) developed the hydraulic and travel time-equivalent technique which is used in this work as described below. To determine the equivalent pipe, the equivalent diameter of the aggregated pipes is first determined using the average total travel time of series and parallel pipes. The average total travel time across a set of series pipes is the sum of the travel times in each pipe. For parallel pipes, the total travel time is determined by discharge-weighted average travel time. Whereas the computed equivalent length ensures that the travel time in the equivalent pipe will equal to the series or parallel pipes, it does not ensure that the system will be hydraulically equivalent. To maintain hydraulic consistency between the original and equivalent systems, pipe roughness is determined from equivalent pipe relationships derived using conservation of energy across a set of pipes in parallel or series. In this work, the expression derived from the Manning's equation is used to calculate the equivalent length (Habibi 2017, Raczynski et al. 2008).

For derivation of the ESDN, it is necessary first to determine the flow directions of the real network. For this purpose, an automatic algorithm has been newly developed in R. The program inputs the GIS layers of inlets, junctions, outlets and pipe identifiers and coordinates, and outputs flow directions in the real storm drain network. The algorithm starts from the most downstream point of the network and moves upstream in the following sequence of operations:

1. Select an outfall from the outfall GIS layer;
2. Identify all pipes that drain to the selected outfall;
3. Determine the flow direction for each pipe identified in Step 2 based on elevation; and
4. Locate the immediate upstream point and repeat Steps 2 and 3.

The flow directions derived above for the actual storm drain network are used to derive the equivalent network using a second automatic algorithm developed in R which is described below:

1. Select an outfall in the real network and read flow directions for the branch of the actual network that drains to the outfall;
2. Select the most upstream grid box in the branch and search for any connecting pipes;
3. Calculate the equivalent pipe characteristics;
4. Repeat Steps 2 and 3 until the actual pipes within the grid box are reduced to a single equivalent pipe;

5. Repeat Steps 2 through 4 for all grid boxes that contain the branch until the outlet is reached; and
6. Repeat the above steps for all branches within the real network.

For the algorithmic details, the reader is referred to Habibi (2017). Figs 2a and 2b show the original storm drain network and the resulting equivalent network for the five urban catchments on a 250 m grid, respectively. In these catchments, there are about 22,000 storm drain pipes and open channels in the actual network which are reduced to about 2,000 in the equivalent network. Some storm drain open channels are self-contained and are not connected to any other structures. Such channels are considered as natural channels and excluded in the construction of the ESDN. To check the goodness of the equivalent network modeling, the routing results using the full and equivalent networks for the Johnson Creek Catchment (see Fig 3) are compared in Fig 4 at the outfalls of six branches of the equivalent network. For routing, kinematic wave model is used for both networks using the same inflows (see Subsection 2.5). Fig 4 shows that the hydrographs from the equivalent network are very close to those from the original network. The comparisons are similar for the other catchments and are not shown. The above results indicate that the equivalent network represents the storm drain network very well.

The ESDN identified in this way is then connected to the natural channel network by mapping the former in HRAP coordinates and assigning cell numbers that are common to both the natural channel and the equivalent storm drain networks. Missing values of slope and diameter for storm drains exist in the storm drain database provided by the Cities of Arlington and Grand Prairie. In this work, they are filled with estimates according to the following rules. If the pipe diameter is unknown, the pipe size is selected based on the standard pipe size chart and the sizes of the up- and downstream pipes. If the slope of the pipe is unknown, the ground slope is used.

2.4 Flow into storm drains

Flow into the ESDN is determined by modeling inlet flows under the following assumptions:

1. Runoff generated on the inlet-bearing roadways drains first into the ESDN, based on head-discharge inlet equations and provided that the sewer network is not full,
2. If the storm drain network is full, the runoff drains into the natural channel in that grid box, and
3. All inlets in the same grid box share the same capacity.

There are four types of inlets typically used for urban drainage: curb opening, grate, and combination (of curb opening and grate) inlets and linear drains (Akan and Houghtalen 2003, TxDOT 2016). In the study area, curb opening inlets dominate. It is therefore assumed that all inlets are of this type. Weir or orifice equations have been used by many researchers to determine flow rate into a curb inlet. Fig 5 shows the flow rate as a function of water depth for three different inlet lengths (see Subsection 4.4 for the choice) for the same inlet height and discharge coefficient based on Leandro et al. (2007), Chen et al. (2003), Gallegos et al. (2009) and TxDOT (2016). Changing the inlet height or discharge coefficient has the same effect as changing the inlet length (see Eqs.(5) and (6) below). As such, Fig 5 depicts the sensitivity to inlet height or discharge coefficient as well. The figure indicates that significant variations exist among different models, and that TXDOT (2016) overlaps the most with the other models. In this work, TXDOT (2016) was used as described below. Clogging is accounted for by fractionally reducing the number of inlets in a grid box (see Subsection 4.4). Other factors that may also modify inlet flow (see, e.g., Leitão et al. 2016) are not considered in this work for simplicity.

If the depth of flow in the gutter is less than or equal to 1.4 times the height of the inlet opening, the inlet is assumed to operate as a weir (TxDOT 2016). If there are N_w such inlets in the grid cell, the total flow into the ESDN at that grid box is given by (TxDOT 2016):

$$Q_{inlet} = N_w C_w L_w y^{3/2} \quad if \quad y \leq 1.4d \tag{5}$$

where Q_{inlet} denotes the flow into the ESDN (m^3/s), C_w denotes the weir coefficient of 1.6 ($m^{0.5}/s$), L_w denotes the length of the curb inlet opening (m), y denotes the water depth at the inlet opening (m), and d denotes the height of the inlet opening (m). If y > d, the inlet is assumed to operate as an orifice. Note that the water depth y in Eq.(5) reflects the slope of the pavement from which the pavement flow drains into the inlet (see Eqs.(8)). The total flow through N_o such orifices is given by (TxDOT 2016):

$$Q_{inlet} = N_o C_o d L_o \sqrt{2gy} \quad if \quad y > d \tag{6}$$

where C_o denotes the orifice coefficient of 0.67, L_o denotes the circumference of the orifice (m), and g denotes the gravitational acceleration (m/s^2). At depths between 1.0 and 1.4 times the opening height, flow is in a transition stage and is determined based on the smaller of the weir and orifice flows.

To determine y in Eqs.(5) and (6), water depth on the pavement in each grid box was modeled using kinematic wave routing analogous to that for hillslope routing in Eqs.(1) and (2):

$$\frac{\partial h_{pvmt}}{\partial t} + L_{pvmt} \frac{\partial q_{pvmt}}{\partial x} = i \tag{7}$$

$$q_{pvmt} = \frac{1}{L_{pvmt}} \frac{1}{n_{pvmt}} h_{pvmt}^{5/3} S^{1/2} \tag{8}$$

where h_{pvmt} denotes the water depth on the pavement (m), i denotes the rain rate for the grid cell (m/s), q_{pvmt} denotes the flow on the pavement per unit area (m/s), L_{pvmt} denotes the pavement length (m) assumed to be $\sqrt{f_c}$ (m) and n_{pvmt} denotes the Manning's roughness coefficient for the pavement. The total flow from the pavement area in a grid box, Q_{pvmt} (m^3/s), is given by $Q_{pvmt} = q_{pvmt} f_{pvmt}$ where f_{pvmt} denotes the pavement area (m^2) estimated from the GIS layers. The water depth on the pavement, h_{pvmt}, is used for y in Eqs.(5) and (6). If Q_{inlet} is larger than Q_{pvmt}, Q_{inlet} is set to Q_{pvmt}. If Q_{inlet} is smaller than the total hillslope flow into the channel, $q_{L_h} f_c$, the remaining flow $q_{L_h} f_c - Q_{inlet}$ is assumed to drain into the natural channel as shown in Eq.(3). In the highly unlikely case of $Q_{inlet} > q_{L_h} f_c$, Q_{inlet} is set to $q_{L_h} f_c$. In reality, the curb-opening inlets intercept gutter flow whereas Eqs.(7) and (8) model sheet flow. Also, a number of parameters in the routing and inlet flow models is subject to significant uncertainties. To assess the impact of the parameters to partitioning of surface runoff into flow into the storm drain network and that into the natural channels, a sensitivity analysis was carried out with respect to the key inlet flow model parameters (see Subsection 4.4).

2.5 Storm drain flow modeling

Flow through the ESDN is modeled based on simplification of the continuity and momentum equations under the kinematic wave assumption (Chow et al. 1988):

$$dV/dt = Q_{in} - Q_{out} \tag{9}$$

$$S_f = S_0 \tag{10}$$

where V denotes the volume of water in the pipe (m^3), Q_{in} denotes the inflow rate (m^3/s) and Q_{out} denotes the outflow rate (m^3/s). If the upstream end of the pipe represents an inlet(s), we have

$Q_{in}=Q_{inlet}$. If the downstream of the pipe represents an outfall(s), we have $Q_{out}=Q_{outfall}$. The above simplification is valid if the variations in the hydrograph are gradual enough to result in a quasi-steady flow for each pipe (Motiee et al. 1996) and the pipe is not surcharged. The momentum equation can be expressed via the Manning's equation as (Chow et al. 1988):

$$A_p = \left(\frac{n_p P_p^{2/3}}{S_o^{1/2}}\right)^{3/5} Q_{out}^{3/5} \tag{11}$$

where A_p denotes the wetted cross-sectional area of the pipe (m^2), n_p denotes the Manning coefficient for the pipe, P_p denotes the wetted perimeter of the pipe (m), and S_o denotes the slope of the pipe. In Eq.(11), A_p and P_p are computed from the downstream water depth. For the flowchart of the integrated model operation, the reader is referred to Habibi (2017). Note that, while multiple elements have been newly added as described above, the only change necessary to the RDHM code itself is adding the source and sink terms in Eq.(3).

3 Study area and data used

The study area includes five urban catchments in the Cities of Arlington and Grand Prairie in the Dallas-Fort Worth (DFW) area of TX with a combined area of 144.6 km^2 (see Fig 2). The size and time-to-peak at the outlet of each catchment vary from 3.4 to 54.6 km^2 and from 0.5 to 2.5 hrs, respectively (Rafieeinasab et al. 2015). For the storm drain network and topography in the study area and the percent impervious cover, the reader is referred to Rafieeinasab et al. (2015). The average percent impervious cover varies from 31% in the Fish Creek Catchment to 48% in the Johnson Creek Catchment.

For the RDHM, a total of 11 a priori parameters for the SAC are available for the CONUS at 1 HRAP resolution based on soil and land cover data (Anderson et al., 2006; Zhang et al., 2011).

In this work, the SAC parameters were derived at a resolution of 1/16 HRAP for the study area (Norouzi 2016) using the computer program developed by the NWS (Zhang et al. 2011). The soil and land cover data used are from the Soil Survey Geographic (SSURGO) database and the National Land Cover Database (NLCD) for 2001, 2006 and 2011, respectively. In addition to the 11 a priori parameters, PCTIM (Permanently Impervious Area) was also derived for the study area at 1/16 HRAP resolution for the SAC which assumes that all rain that falls on the impervious area runs off without interception storage.

To evaluate the performance of the integrated model, streamflow simulations were compared with observations. For the study basins, water level observations from pressure transducer sensors are available every 15 min from the high water warning system operated by the Cities of Arlington and Grand Prairie. These observations were used previously to validate streamflow simulations (Rafieeinasab et al., 2015a) using rating curves derived via 1-D steady state non-uniform hydraulic modeling (Kean and Smith 2005, 2010; Norouzi et al. 2015).

High spatiotemporal-resolution Quantitative Precipitation Estimation (QPE) is essential for prediction of urban flash floods. For the study area, the DFW Demonstration Network of the Collaborative Adaptive Sensing of the Atmosphere (CASA) Program consisting of high-resolution X band radars provides high resolution (500 m, 1 min) QPE (Chen and Chandrasekar 2015) which also utilizes the Next-Generation Radar (NEXRAD). Rafieeinasab et al. (2014, 2015) carried out comparative evaluation of different radar-based QPE products for the study area. They showed that, in general, the CASA QPE is more accurate for larger precipitation amounts whereas the Multisensor Precipitation Estimator (MPE, Seo et al. 2010) estimates are more accurate for smaller amounts. In this work, both the CASA and MPE QPE products are used.

4 Results

This section presents the results in four parts: 1) comparison of the simulated flow at catchment outlets against observations to assess the ability of the model to well represent real flows in the natural channels; 2) analysis of the integrated model results with and without storm drain modeling from site to catchment scales to assess the contributing area-dependent impact of storm drains to surface flow; 3) assessment of the impact of storm drains on peak flow under the existing land cover conditions and under a 15% increase in imperviousness; and 4)assessment of the impact of the initial conditions of the storm drain flow model and the sensitivity of the conveyance volumes in the natural channel and storm drain networks to selected inlet flow model parameters.

4.1 Comparison with observed flow at catchment outlet

The ESDN modeled in this work include not only the storm drainage pipes but also the open channel to which storm drainage pipes are connected. All other man-made open channels, not including roadways, are considered as part of the natural channel network. One may hence expect the conveyance capacity of the ESDN to be relatively modest compared to that of the natural channel network. Rafieeinasab et al. (2015) indicated that full-capacity open channel storm drains can convey several times more flow than full-flow storm drain pipes in the study area, and that, for a large event such as Tropical Storm (TS) Hermine in 2010, the natural channels convey about 3 and 15 times as much flow as the full-capacity man-made open channels and pipes, respectively. TS Hermine produced 160 mm of rainfall over a 24-hr period in the study area which corresponds to a return period of about 25 years. In the study area, water level observations are available only at the catchment outlets where the discharge represents the combined flow through both the natural channels and storm drains. As such, comparison of streamflow at the outlets of sizable catchments is not likely to reveal the impact of storm drains. On the other hand, one may still compare the natural-channel flow simulations with and without storm drain modeling with the observed flow to assess the quality of the integrated model simulation at the catchment scale. The premise of such comparison is that, if the model can simulate outlet flow realistically, it is likely to be able to simulate flows from smaller contributing areas. It is important to note that, in this assessment, we are not necessarily interested in the absolute accuracy of the simulation given the various sources of error. Instead, our primary interest is in ascertaining whether the model response is realistic at the catchment scale relative to the observed flow so that the model response at smaller spatial scales is likely to be realistic.

Figs 6a and 6b show the hyetographs (top) and the simulated vs. observed hydrographs (bottom) for two events occurred in late November and December of 2015, respectively, in the 14.4 km^2 Cottonwood Creek at Carrier (Outlet 6363). The total rainfall amounts are 120 mm over a 24-hr period for the Nov event (Fig 6a) and 90 mm over a 48-hr period for the Dec event (Fig 6b) which correspond to return periods of approximately 5 and 2 years, respectively. Fig 6c shows the comparison of simulated flow vs. observed water level for the Jan 2017 event shown in Fig 10a (see Subsection 4.2) at three additional outlet locations of 6043 (Arbor Creek at Tarrant), 6083 (N Fork Cottonwood at GSWP) and 6143 (Fish Creek at GSWP); the contributing areas are 4.1, 8.4 and 31.2 km^2, respectively. The rainfall data used is the CASA QPE at 1/8 HRAP and 1-min resolution. The RDHM resolution is at 1/16 HRAP. Figs 6a and 6b indicate that the model simulations are able to capture the events quite well, but that they are not able to pick up very fast-varying streamflow responses very well. In addition, the model simulation for the late Dec event exhibits flow magnitude-dependent errors. The errors present in these simulations are not at all surprising in that they are based solely on the a priori model parameters for both soil moisture accounting and routing as no calibration was attempted in this work. Overall, it is seen that the model is capable of producing realistic streamflow responses to significant rainfall events albeit with a mix of both amplitude (Seo et al. 2009) and phase (Liu et al. 2011) errors of varying magnitude. Comparison of streamflow simulations with (red dashed line) and without (blue dashed line) storm drain modeling in Fig 6a indicates that the differences between the two are indistinguishable for the larger Nov event, but that, for the smaller Dec event, the peak flows at the outlet have increased slightly with storm drain modeling. Fig 6c, which only allows qualitative comparison of flow vs. stage, generally supports the above observations. Fig 6c indicates that, for Outlet 6143 which is associated with the largest contributing area among the four, significant hydrologic uncertainty exists which is likely to override the effects of storm drain modeling except perhaps for the most upstream areas. As explained above, discharge at the catchment outlet reflects both the natural channel and storm drain flows and hence is not very useful in assessing the impact of storm drains. To assess performance at much smaller spatial scales, a set of twin simulation experiments were carried out which is described below.

4.2 Impact of storm drains at different scales of contributing area

In the DFW area, the design of stormwater infrastructure calls for 25-yr 24-hr design rainfall for conveyance, and for 100-yr 24-hr design rainfall for flood mitigation (NCTCOG 2015). In this work, we apply spatially uniform 100-yr 5-min and 24-hr rainfall of constant rates to assess the impact of storm drain network on channel flow in response to impulse- and step-function forcings of rainfall, respectively. We then apply two actual events for additional assessment. Fig 7 shows the simulated hydrographs of channel flow with (red solid line) and without (blue solid line) SDM at all grid boxes in the Johnson Creek Catchment (Outlet 6033, 40.4 km^2) due to a spatial uniform rainfall pulse of 280.7 mm/hr lasting 5 min. Because the hydrographs shown in the figure represent the response of the contributing areas to what is essentially an impulse, they may be considered as scaled unit hydrographs. As expected, the smaller the contributing area, the faster the hydrologic response. Though difficult to see in this figure, there are numerous hydrographs near the origin representing the response of very small contributing areas. To help discern the hydrographs associated with storm drains from those without, Fig 8 shows the box-and-whisker plots of the surface flow in logarithmic scale at all grid boxes as a function of time elapsed with and without SDM. In the figure, the upper and lower ends of the box represent the 75^{th} and 25^{th} percentiles, the line in the box represents the median, and the ends of the whiskers represent median $\pm 1.58 \times IQR/\sqrt{N}$ where IQR denotes the inter-quartile range and N denotes the sample size. It is seen that the storm drains in this catchment reduce surface flow in the median sense for about 30 min, and that at a number of locations the reduction persists well past 30 min. For Outlet 6133 of the Fish Creek Catchment (54.3 km^2, not shown), it was observed that the storm drains reduce flow at most locations only for the first 10 min or less, and that between 15 and 40 min or so there is a noticeable increase in flow with storm drains modeled. The above observations suggest that the Fish Creek Catchment may be susceptible to downstream flooding due to storm drains upstream. To track the impact of storm drains on surface flow at each grid box during the course of the catchment response following an impulse rainfall, Fig 9 plots the ratio of the flow with storm drains to that without at all grid boxes in the Johnson Creek

Catchment due to 100-yr 5-min rainfall. A ratio of less or greater than unity is an indication that the storm drains reduce or increase surface flow at that location, respectively. Note in the figure that the storm drains reduce flow significantly for a very short duration at almost all grid cells, that the flow remains reduced for the entire duration at many of the above locations, but that there are locations where the storm drains increase flow between 5 to 50 min. The results for other catchments are qualitatively similar and are not shown. Figs 10a and 10b show the hyetographs and box-and-whisker plots of the hydrographs with and without SDM for the Johnson Creek Catchment (GP6033) for the Jan 16, 2017, and May 29, 2015 events, respectively. Also shown are the rainfall maps based on the CASA QPE. The 2017 event, a fast-moving convective front which also spawned tornadoes, produced up to 100 mm of rain in about 6 hours in parts of the catchment. The 2015 event, which was the largest in DFW during the wettest ever May of that year, produced up to 130 mm in about 7 hours in large parts of Arlington and Grand Prairie. For the Jan 2017 event, it is seen that the storm drains reduce surface flow significantly, and that at many locations the reduction persists throughout the event. For the May 2015 event, which had a return period of over 300 years for 6-hr duration (Norouzi 2016), the storm drains had a very small impact as the extreme rainfall was widespread and quickly filled almost the entire storm drain network (Fig 10b). For stormwater planning and management, the locations where surface flow increases due to storm drains are of particular interest. The following subsection describes how such areas may be identified by spatially mapping the changes in peak surface flow from the integrated model.

4.3 Impact of storm drains on peak flow

To ascertain the locations where storm drains may increase or decrease peak surface flow, the ratio of the peak flow with storm drains to that without is calculated at each grid cell and mapped over the entire catchment. This ratio is referred to herein as the peak flow ratio (PFR). Fig 11 shows the map of the PFR for a 100-yr 24-hr rainfall amount of 280.7 (mm) for the entire study area. Note in the figure that the PFR is less than unity for most cells (i.e. storm drains reduce peak flow), and that the ratio is smaller for many grid cells where a large number of inlets exist. Fig 12 shows the map of the PFR exceeding unity but only for those cells that do not contain outfalls. In this way, we exclude the cells from consideration where the increase in peak flow is due to direct discharges from storm drains. It is likely that some of the colored cells shown in Fig 12 contain higher-order natural streams for which the performance of storm drain systems may not be of concern. All other colored cells in Fig 12 may be considered as not being served well by the existing stormwater infrastructure in the sense that peak flow has increased due to storm drains compared to the storm drain-less conditions.

In the DFW area and elsewhere, continuing urbanization is expected to alter the hydrologic response of urban catchments. Analysis of the NLCD land cover of 2001, 2006 and 2011 for the area indicates that imperviousness increased by about 15 percent between 2001 and 2011 (Norouzi 2016). Fig 13 is the same as Fig 11 but the peak flow with storm drains under the existing condition (i.e., the denumerator in the PFR) has been replaced with that under a uniform 15% increase in imperviousness in all catchments. Note that, with the increase in imperviousness, the size of the area of the PFR exceeding unity has increased by about 30%, indicating that in many areas the existing storm drains would no longer be adequate.

4.4 Sensitivity to initial conditions of storm drain flow and inlet flow parameters

Because the residence time of stormwater in the storm drain network is only of the order of 10 hours or less for the study catchments, in most situations one may safely initialize the ESDN with no-flow conditions. As the event progresses, however, the accuracy of the model state may deteriorate due to the growth of simulation error in time. It is hence necessary to assess the impact of the initial flow conditions in the ESDN on time-to-peak and peak flow. To that end, comparisons of time-to-peak and peak flow were made between the two bounding conditions of completely empty and full storm drains following a 100-yr return period rainfall of 5-min duration. The results indicate that the accuracy of the state variable in the storm drain model, A_p in Eq.(11), may impact the quality of simulation significantly, particularly when the storm drains may undergo successive cycles of filling and draining from successive short-duration pulses of rainfall.

Although flow through storm drain systems is well understood, its modeling entails significant uncertainties (Pappenberger et al. 2008; Mantovan and Todini, 2006). In this work, inlet flows are determined based on uniform kinematic-wave water depth over the paved areas in each grid cell assuming either weir or orifice flow (see Subsection 2.4). In reality, inlet flow is partitioned from gutter flow whose depth is typically larger than the uniform water depth over the entire pavement. In inlet design, inlet flow is determined by the interception rate, or the efficiency of the inlet, which depends on the gutter flow (TxDOT 2016). In this work, we assess the impact of selected inlet parameters to partitioning of hillslope runoff into inlet and channel flows by evaluating the sensitivity of weir flow in Eq.(5) to the inlet length, L_w. Because changing the number of inlets in the grid cell, N, or the weir coefficient, C_w, has the same effect as changing L_w, analysis of sensitivity on L_w amounts to that of all three parameters, N, C_w and $L_{w.}$ For this reason, we chose a wide range of values for L_w to encompass possible variations in N and C_w as well. In the study area, both curb-opening and depressed curb-opening inlets exist for which the weir discharge coefficient, C_w, is 0.374 and 0.286, respectively. A typical curb-opening inlet has a length of 2.5 m in the study area but, at many locations, the inlets are doubled to a length of 5.0 m. Inlets may be clogged which would effectively reduce N and/or L_w. In inlet design, clogging factors of 0.12 and 0.08 are suggested for one and two units of curb-opening inlets (Guo and MacKenzie 2012) which effectively reduces N in Eq.(5) to 0.88N and 0.92N, respectively. From the above, one may arrive at the lower and upper bounds for NC_wL_w of 0.63N and 1.87N, respectively. To encompass approximately the above range of possible variations, L_w=1.7, 2.5 and 5.0 (m) were chosen without reducing N and keeping C_w=0.374. Then L_w=10.0 (m) and 50.0 (m) were added to assess the asymptotic behavior. Fig 14 shows the volume of stormwater conveyed by the natural channels vs. the storm drains from spatially uniform 100-yr return period 5-min rainfall over the five catchments. The uppermost dotted black line denotes the total stormwater volume conveyed both by the natural and storm drain networks. Different colors represent different nominal inlet lengths. For each color, the solid and dashed lines denote the stormwater conveyed by the natural channels and storm drains, respectively. The solid and dotted lines of the same color hence partition the total stormwater volume into natural channel and stormwater flow volume. The following observations may be made in Fig 14. The stormwater volume conveyed by storm drains with a nominal inlet length of 2.5 and 5.0 m is approximately 22 and 38%, respectively, of the total runoff volume for both 5-min and 24-hr rainfall of 100-yr return period. The limiting conveyance volume by storm drains is reached at the nominal inlet length of 50 m where over 60% of the surface runoff is conveyed by storm drains. As expected, the rate of increase in the runoff volume conveyed by storm drains decreases as the nominal inlet length increases, i.e., there is diminishing marginal value in increasing the inlet capacity. The above results indicate that significant uncertainties exist in partitioning surface runoff into natural channel and storm drain flows, and that rigorous uncertainty analysis is necessary for comprehensive assessment. With greatly reduced modeling complexity and computational requirements, the integrated modeling approach proposed in this work makes such analysis readily possible. Currently, simulation of a 24-hr event for the study area of 144.6 km^2 at a 250-m resolution with 1-min rainfall input takes about 3 hours (or about 12.5 seconds per time step) on a 6 Intel® Xeon® CPU E5-2620 v2 @ 2.10GHz core computer with 65 GB memory. The current version of the storm drain model has very large room for improvement in computational efficiency. It is expected that multi-fold and significant reduction in computing time is readily achievable with and without parallelization, respectively, a task left as a future endeavor.

5 Conclusions and future research recommendations

For accurate flash flood forecasting and effective stormwater planning and management in urban areas, it is necessary to model not only the natural channel systems but also the large and complex networks of storm drains. Whereas there exist many 1D-2D models, most are not well-suited for real-time operation or large-area implementation due to extremely large computational and modelling requirements (Noh et al. 2018). High-resolution distributed modelling, on the other hand, is now a common operational practice for water modelling and forecasting for large areas (>100 km^2) around the world (see, e.g., the National Water Model (NWM) in the US, http://water.noaa.gov/about/nwm). In this work, we propose a modular storm drain model which may be easily coupled with existing gridded distributed hydrologic models. The proposed integrated model is applied to a 144.6 km^2 area consisting of five urban catchments in the Cities of Arlington and Grand Prairie in Texas, US. Whereas the above domain is large by the stormwater modeling standards, it represents only a small fraction of the large cities in DFW. For reference, the Cities of Dallas, Fort Worth, Arlington and Grand Prairie which comprise the mid-section of DFW have a combined area of about 2,371.9 km^2. The storm drain module described in this work is aimed at eventual operation for such large areas. A salient feature of the proposed approach is the use of the equivalent storm drain network (ESDN) which approximates the actual storm drain network on the same grid as the distributed hydrologic model, thus rendering coupling of the storm drain module and the distributed model extremely simple. The ESDN uses the equivalent systems method of Raczynski et al. (2008) which has also been used by a number of researchers and practitioners for modelling flow through pipe networks (Mohammad and Ahmad 2011, Gad and Mohammad 2014, Choi and Kang 2015). The gridded distributed hydrologic model used in this work is the NWS's RDHM. The main findings are as follows.

The ESDN represents the real storm drain network very well. At the catchment scale, the impact of storm drains is not readily discernable because streamflow at the catchment outlet integrates both the natural channel and storm drain flows. For smaller catchments, it is seen that storm drain modeling increases peak flow at the outlet slightly for significant events. To assess the impact of the storm drain network at all locations, twin simulation experiments were carried out in which the integrated model was run with and without the storm drain module using impulse- and step-function design rainfall. The results show that the storm drains are very effective in reducing surface flow for a short duration at almost all grid cells in the study area, and that, at many locations, the flow remains reduced for the entire duration. For the highly urbanized Johnson Creek Catchment (Outlet 6033), the storm drain network reduces surface flow at most locations for about 30 min, and that the reduction persists well past 30 min at many locations. For the least impervious Fish Creek Catchment (Outlet 6133), on the other hand, the storm drain network reduces surface flow only for the first 10 min or less at most locations, and increases noticeably between 15 and 40 min. The above suggests that the Fish Creek Catchment may be susceptible to downstream flooding due to storm drain flow from upstream. The simulation results also reveal that there are locations in the Johnson Creek Catchment where the existing storm drain network may increase peak flow compared to the storm drain-less conditions, and that, with a 15% increase in imperviousness relative to the current conditions, the existing stormwater infrastructure would lose effectiveness for approximately 30% of the study area. The above results demonstrate the potential power of the integrated model for real-time flash flood forecasting as well as planning and management of stormwater infrastructure for large urban areas.

The integrated model simulations also show that for the study area the stormwater volume conveyed by storm drains with a nominal inlet length of 2.5 and 5.0 m is approximately 22 and 38%, respectively, of the total runoff volume for both 5-min and 24-hr rainfall of 100-yr return period. As expected, the rate of increase in the runoff volume conveyed by storm drains decreases as the nominal inlet length of the inlet increases, indicating diminishing marginal value in increasing the inlet capacity. The sensitivity to the inlet flow parameters indicates significant uncertainties in partitioning surface runoff into natural channel and storm drain flows. Whereas rigorous uncertainty analysis for stormwater infrastructure for a large area using 1D-2D modeling would be extremely expensive for modeling and computationally-wise, the integrated modeling approach proposed in this work makes such analysis possible even for very large areas.

Due to the coarse resolution and simplifications, however, the proposed approach cannot resolve flow at sub-grid scales and hence is not suitable for very detailed modeling for small areas.

Validation of simulation results at sufficiently small spatial scales remains a large challenge due to lack of ubiquitous streamflow sensing. It is noted that water level sensors are being deployed at small urban streams in the study area and elsewhere in DFW (Habibi et al. 2017) and the crowdsourcing app, iSeeFlood (Choe et al. 2017, http://ispuw.uta.edu/nsf/8-1-1description.html), have also been launched to aid validation as well as real-time forecasting. The NWS has recently implemented NWM (Graziano et al. 2017), a hydrologic model that uses the Weather Research and Forecasting Model Hydrological modeling system (WRF-Hydro, Gochis et al. 2014), to forecast streamflow and other hydrologic variables over CONUS. Though WRF-Hydro and RDHM have significant differences in routing operations, it is expected that the storm drain module developed in this work can also be integrated with WRF-Hydro with a modest amount of effort (David Gochis, personal communication, May 2017).

Acknowledgments

This material is based upon work supported by the National Science Foundation under Grant No. CyberSEES-1442735 and by the National Oceanic and Atmospheric Administration's Joint Technology Transfer Initiative Program under Grant NA17OAR4590184. These supports are gratefully acknowledged. We would like to thank Dr. Zhengtao Cui of the NWS Office of Water Prediction for help with RDHM modeling, Mses. Amy Cannon of the City of Arlington and Stephanie Griffin of the City of Grand Prairie for providing the storm drain and related data used in this work.

References

Akan, A. O. and Houghtalen, R. J., 2003. Urban hydrology, hydraulics, and stormwater quality: engineering applications and computer modeling. John Wiley & Sons.

Andersen, H. S., Tamašauskas, H., Mark, O., 2004. The full urban water cycle – modeling with MIKE URBAN. 7th Urban Drainage Modelling, Dresden, Germany.

Anderson, E. J. and Al-Jamal, K. H., 1995. Hydraulic-network simplification. Journal of water resources planning and management, 121(3), pp.235-240.

Anderson, R. M., V. Koren and S. M. Reed., 2006. Using SSURGO Data to Improve Sacramento Model A Priori Parameter Estimates. Journal of Hydrology 320 (1): 103–16.

Arnbjerg-Nielsen, K., Willems, P., Olsson, J., Beecham, S., Pathirana, A., Gregersen, I. B., Madsen, H. and Nguyen, V.T.V., 2013. Impacts of climate change on rainfall extremes and urban drainage systems: a review. Water Science and Technology, 68(1), pp.16-28

Bonnifait, L., Delrieua, G., Laya, M. L., Boudevillaina, B., Massonb, A., Belleudya, P., Gaumec, E., Saulnier, G. M., 2009. Distributed hydrologic and hydraulic modelling with radar rainfall input: Reconstruction of the 8–9 September 2002 catastrophic flood event in the Gard region, France. Adv. Water Resour. 32, 1077–1089

Burnash, R. J. C., Ferral, R. L., and McGuire, R. A., 1973. A Generalized Streamflow Simulation System: Conceptual Modeling for Digital Computers. US Department of Commerce National Weather Service and State of California Department of Water Resources.

Chen, A. S., Evans, B., Djordjević, S. and Savić, D. A., 2012. Multi-layered coarse grid modelling in 2D urban flood simulations. Journal of Hydrology, 470, pp.1-11

Chen, S. H., Hsu, M. H. and Chen, T. S., 2003. Simulation for interactions between storm sewer and overland flows. In New Pipeline Technologies, Security, and Safety (pp. 437-446).

Chen, H, and Chandrasekar, V., 2015. The quantitative precipitation estimation system for Dallas-Fort Worth (DFW) urban remote sensing network. J. Hydrol. 531,259–271.

Choe, C., Seo, S., Sreetharan, S., 2017. Real-time, Crowd-Sourced Flood Mapping & Analytics via iSeeFlood. Paper presented at the meeting of New York State Floodplain and Stormwater Managers Association Conference, Binghamton, New York.

Choi, J. and D. Kang, 2015. Assessment of skeletonization techniques for water distribution systems. Korea Water Resources Association, 48(10): 845-855.

Chow, V. T., Maidment, D. R. and Mays, L. W., 1988. Applied Hydrology. New York: McGraw-Hill.

David, C. H., Maidment, D. R., Niu, G. Y., Yang, Z. L., Habets, F. and Eijkhout, V., 2011. River Network Routing on the NHDPlus Dataset. Journal of Hydrometeorology 12:913–34.

Denault, C., Millar, R. G., and Lence, B. J. 2006. Assessment of possible impacts of climate change in an urban catchment. J. Am. Water Resour. Assoc., 42(3), 685–697.

DHI, 1995. Mouse: User's manual and tutorial, Danish Hydraulic Institute, Horsholm, Denmark.

Duncan, A., Chen, A.S., Keedwell, E., Djordjevic, S. and Savic, D., 2011. Urban flood prediction in real-time from weather radar and rainfall data using artificial neural networks

Emerson, C. H., Welty, C., and Traver, R. G., 2005. Watershed-scale evaluation of a system of stormwater detention basins, J. Hydrol. Eng., 10, 237–242.

Fares, A., Awal, R., Michaud, J., Chu, P. S., Fares, S., Kodama, K. and Rosener, M., 2014. Rainfall-runoff modeling in a flashy tropical watershed using the distributed HL-RDHM model. Journal of hydrology, 519, pp.3436-3447.

Gad, A.A. and Mohammed, H.I., 2014. Impact of pipes networks simplification on water hammer phenomenon. Sadhana, 39(5), pp.1227-1244

Gires, A., Giangola-Murzyn, A., Abbes, J. B., Tchiguirinskaia, I., Schertzer, D. and Lovejoy, S., 2015. Impacts of small scale rainfall variability in urban areas: a case study with 1D and 1D/2D hydrological models in a multifractal framework. Urban Water Journal, 12(8), pp.607-617.

Gochis, D. J., Yu, W., Yates, D. N., 2014. The WRF-Hydro model technical description and user's guide, version 2.0. NCAR Technical Document Available at: https://www.ral.ucar.edu/projects/wrf_hydro (last access Feb 2017).

Graziano, T., Clark, E., Cosgrove, B., and Gochis, D., 2017. Transforming National Oceanic and Atmospheric Administration (NOAA) Water Resources Prediction, AMS Meeting, Seattle, WA.

Greene, D. R., and Hudlow, M. D., 1982: Hydrometeorological grid mapping procedures. AWRA Int. Symp. Hydrometeorology, AWRA, Bethesda, MD

Guidolin, M., Duncan, A., Ghimire, B., Gibson, M., Keedwell, E., Chen, A. S., Djordjevic, S. and Savic, D., 2012. CADDIES: a new framework for rapid development of parallel cellular automata algorithms for flood simulation.

Guo, J. C. Y., MacKenzie, K., 2012. Hydraulic efficiency of grate and curb-opening inlets under clogging effect. Colorado department of transportation DTD applied research and innovation branch. CDOT-2012-3. Denver, CO, 84pp.

Guo, Y. P., 2006. Updating rainfall IDF relationships to maintain urban drainage design standards. J. Hydrol. Eng., 11(5), 506–509.

Habibi, H., 2017. Integrated modeling of storm drain and natural channel networks for real-time flash flood forecasting and stormwater planning and management in large urban areas, PhD dissertation, Dept of Civil Eng, The University of Texas at Arlington.

Habibi, H., B. Nazari, A. Norouzi, S. Noh, D.-J. Seo, S. Sinha, X. Yu, M. Bartos, B. Kerkez, L. Lakshman, M. Zink, E. Lyons, B. J. Philips, P. Jangyodsuk, and J. Gao, 2017. 2A.1 Integrated Sensing and Prediction of Flash Floods for the Dallas-Fort Worth Metroplex (DFW), AMS Meeting, Seattle, WA.

Habibi, H., Nasab, A. R., Norouzi, A., Nazari, B., Seo, D.-J., Muttiah, R., & Davis, C., 2016. High Resolution Flash Flood Forecasting for the Dallas-Fort Worth Metroplex. Journal of Water Management Modeling.

Hénonin, J., B. Russo, D. S. Roqueta, R. S. Diezma, N. D. S. Domingo, F. Thomsen, and O. Mark, 2010. Urban flood real-time forecasting and modelling: A state-of-theart review, MIKE by DHI Conference, Sep 6-8, Copenhagen, Denmark.

Huber, W. C., and Dickinson, R. E., 1988. Stormwater management model user’s manual, version 4, EPA/600/3-88/001a (NTIS PB88- 236641/AS), Environmental Protection Agency, Athens, Ga.

Innovyze, 2012. InfoWorks ICM (Integrated Catchment Modeling) v.2.5. User manual references.

Jeppson R. W., 1974. Steady flow analysis of pipe networks: an instructional manual. Department of Civil Engineering and Utah Water Research Laboratory, College of Engineering, Utah State University, Logan, Utah.

Kean, J. W., and Smith, J. D., 2010. Calculation of stage-discharge relations for gravel belled channels. Journal of Geophysical Research-Earth Surface, 115.

Kean, J. W., Smith, J. D., 2005. Generation and verification of theoretical rating curves in the Whitewater River Basin, Kansas. J. Geophys. Res., 110.

Kim, J., Warnock, A., Ivanov, V. Y., Katopodes, N. D., 2012. Coupled modeling of hydrologic and hydrodynamic processes including overland and channel flow. Adv. Water Resour. 37, 104–126.

Koren, V., Reed, S., Smith, M., Zhang, Z., and Seo, D.-J., 2004. Hydrology laboratory research modeling system (HL-RMS) of the US national weather service. Journal of Hydrology, 291(3), 297-318.

Larock et al., B. E., Jeppson, R.W., Watters, G. Z., 2000. Hydraulics of Pipeline systems. CRC Press, Boca Raton, Florida.

Leandro, J., Chen, A., Djordjevic, S. and Savic, D., 2009. A comparison of 1D/1D and 1D/2D coupled hydraulic models (sewer/surface) for urban flood simulation. Journal of Hydraulic Engineering, 135(6), 495-504.

Leandro, J., Djordjevic, S., Chen, A. S. and Savic, D., 2007. The use of multiple-linking-element for connecting sewer and surface drainage networks. In Proceedings of the Congress-International Association for Hydraulic Research (Vol. 32, No. 1, p. 204).

Leitão, J. P., Simões, N. E., Pina, R. D., Ochoa-Rodriguez, S., Onof, C. & Sá Marques, A. (2016). Stochastic evaluation of the impact of sewer inlets' hydraulic capacity on urban pluvial flooding. Stochastic Environmental Research and Risk Assessment.

Leitão, J. P., Simões, N. E., Maksimović, Č., Ferreira, F., Prodanović, D., Matos, J. S. and Marques, A. S., 2010. Real-time forecasting urban drainage models: full or simplified networks?. Water Science and Technology, 62(9), pp.2106-2114.

Liu, Y., J. Brown, J. Demargne, and D.-J. Seo, 2011. A wavelet-based approach to assessing timing errors in hydrologic predictions, J. Hydrol., 397(3-4), 210-224.

Mantovan, P. and Todini, E., 2006. Hydrological forecasting uncertainty assessment: Incoherence of the GLUE methodology. Journal of hydrology, 330(1-2): 368-381.

Mailhot, A., Duchesne, S., Rivard, G., Nantel, E., Caya, D., and Villeneuve, J. P., 2006a. “Climate change impacts on the performance of urban drainage systems for southern Québec.” Proc., EIC Climate Change Technology Conference, Engineering Institute of Canada, Ottawa.

McCuen, R. H., 1979. Statistical terminology: definitions and interpretation for flood peak estimation. Journal of the American Water Resources Association, 15: 1106–1116. doi:10.1111/j.1752-1688.1979.tb01089.x

Moreda, F., Koren, V., Zhang, Z., Reed, S., and Smith, M., 2006: Parameterization of distributed hydrological models: Learning from the experiences of lumped modeling. J. Hydrol., 320, 218–237.

Motiee, H., 1996. Un-modèle numérique pour la simulation des réseaux d'assainissement pluvial fondésur le concept de stockage. Ph.D. Thesis. Lyon, France: Institut National des Sciences Appliquées de Lyon.

Mohamed, H.I. and Ahmed, S.S., 2011. Effect of simplifying the water supply pipe networks on water quality simulation. Inter. Confer. for Water, Energy Environ, 41-46.

Nazari, B., Seo, D.J. and Muttiah, R., 2016. Assessing the Impact of Variations in Hydrologic, Hydraulic and Hydrometeorological Controls on Inundation in Urban Areas. Journal of Water Management Modeling.

Neal, J.C., Schumann, G., Bates, P.D., 2012. A subgrid channel model for simulating river hydraulics and floodplain inundation over large and data sparse areas. Water Resour. Res. 48 (11), 16W11506.

Nguyen, P., Sorooshian, S., Hsu, K., AghaKouchak, A., Sanders, B.F., Smith, M.B. and Koren, V., 2012, December. Improving flash flood forecasting through coupling of a distributed hydrologic rainfall-runoff model (HL-RDHM) with a hydraulic model (BreZo). In AGU Fall Meeting Abstracts.

Nguyen, P., Thorstensen, A., Sorooshian, S., Hsu, K., AghaKouchak, A., Sanders, B., Koren, V., Cui, Z. and Smith, M. (2015). A high resolution coupled hydrologic–hydraulic model (HiResFlood-UCI) for flash flood modeling. Journal of Hydrology.

Norouzi, A., 2016. Evaluation and improvement of fine-scale and hydrologic modeling of large urban areas using hydrometeorological and hydrologic observations. PhD dissertation, Dept of Civil Eng, The University of Texas at Arlington, Arlington, TX.

Norouzi, A., A. Rafieeinasab, D.-J. Seo, J. Lee, 2015. Estimation of Stage-Discharge Relationships in Urban Streams Using a Fluid-Mechanically-Based Model. EWRI Congress, May, Austin, TX.

Norouzi, A., H. Habibi, B. Nazari, S. Noh, D.-J. Seo, Y. Zhang, 2018. Toward Parsimonious Modeling of Frequency of Areal Runoff from Heavy-to-Extreme Precipitation in Large Urban Areas under Changing Conditions – A Derived Moment Approach. Submitted to Stochastic Environmental Research and Risk Analysis.

NWS, 2009. Hydrology Laboratory-Research Distributed Hydrologic Model (HL-RDHM) User Manual v. 3.0.0., National Weather Service Office of Hydrologic Development, Silver Spring, MD.

Noh, S., J. Lee, S. Lee, D.-J. Seo, and K. Kawaike, 2018. Hyper-resolution 1D-2D urban flood modelling using LiDAR data and hybrid parallelization. Environmental Modeling and Software. 103: 131-145. https://doi.org/10.1016/j.envsoft.2018.02.008

Pappenberger, F., Beven, K.J., Ratto, M. and Matgen, P., 2008. Multi-method global sensitivity analysis of flood inundation models. Advances in water resources, 31(1):1-14.

Pina, R. D., Ochoa-Rodriguez, S., Simões, N. E., Mijic, A., Marques, A. S. and Maksimović, Č., 2016. Semi-vs. fully-distributed urban stormwater models: model set up and comparison with two real case studies. Water, 8(2), p.58.

Raczynski A., Kirkpatrick W., Rehnstrom, D., Boulos, P., and Lansey, K, 2008. Developing hydraulic and water quality equivalent systems, Water Distribution Systems Analysis, doi:10.1061/41024(340)73.

Rafieeinasab, A., Norouzi, A., Kim, S., Habibi, H., Nazari, B., Seo, D.-J., Lee, H., Cosgrove, B., & Cui, Z. (2015). Toward high-resolution flash flood prediction in large urban areas–Analysis of sensitivity to spatiotemporal resolution of rainfall input and hydrologic modeling. Journal of Hydrology, 531, 370-388.

Rafieeinasab, A., Norouzi, A., Mathew, T., Seo, D.-J., Chen, H., Chandrasekar, V., Rees, P., and Nelson, B., 2014. Comparative Evaluation of Multiple Radar-based QPEs for North Texas, International Symposium Weather Radar and Hydrology, Apr 7-10, Reston, VA.

Reed, S., Koren, V., Smith, M., Zhang, Z., Moreda, F., Seo, D.-J., and Participants, D. M. I. P., 2004. Overall distributed model intercomparison project results. Journal of Hydrology, 298(1), 27-60.

Reed, S., Schaake, J., Zhang, Z. Y., 2007. A distributed hydrologic model and threshold frequency-based method for flash flood forecasting at ungauged locations. J. Hydrol. 337 (3–4), 402–420.

Reed, S. M., 2003. Deriving flow directions for coarse-resolution (1-4 km) gridded hydrologic modeling. Water Resources Research, 39(9).

Schumann, G. P., Neal, J. C., Voisin, N., Andreadis, K. M., Pappenberger, F., Phanthuwongpakdee, N., Hall, A. C. and Bates, P. D., 2013. A first large-scale flood inundation forecasting model. Water Resources Research, 49(10), pp.6248-6257

Seo, D.-J., Seed, A., and Delrieu, G., 2010. Radar and multisensor rainfall estimation for hydrologic applications. Rainfall: State of the science, 79-104.

Seo, D.-J., L. Cajina, R. Corby and T. Howieson, 2009: Automatic State Updating for Operational Streamflow Forecasting via Variational Data Assimilation, 367, Journal of Hydrology, 255-275.

Simões, N., Ochoa-Rodríguez, S., Leitão, J. P., Pina, R., Sá Marquez, A. and Maksimović, Č., 2011. Urban drainage models for flood forecasting: 1D/1D, 1D/2D and hybrid models.

Smith, M. B., D.-J. Seo, V. I. Koren, S. Reed, Z. Zhang, Q.-Y. Duan, F. Moreda, and S. Cong, 2004: The Distributed Model Intercomparison Project (DMIP): Motivation and experiment design. Journal of Hydrology (DMIP special issue), 298(1-4), 4-26.

Smith, M. B., Koren, V., Zhang, Z., Zhang, Y., Reed, S. M., Cui, Z., Moreda, F., Cosgrove, B.A., Mizukami, N. and Anderson, E.A., 2012. Results of the DMIP 2 Oklahoma experiments. Journal of Hydrology, 418, 17-48.

Soil Conservation Service, 1983. TR-20: Computer programs for projects formulations-hydrology. Tech. Release 20, U.S. Department of Agriculture, Washington, D.C.

Soil Conservation Service, 1986. TR-55: Urban hydrology for small watersheds. Tech. Release 55, U.S. Department of Agriculture, Washington, D.C.

Texas Department of Transportation (TxDOT), 2016. Hydraulic Design Manual, http://onlinemanuals.txdot.gov/txdotmanuals/hyd/hyd.pdf

U.S. Army Corp. of Engineers, 1985. HEC-1: Flood hydrograph package. Hydrologic Engineering Center, Davis, Calif.

Watt, W. E., Waters, D., and McLean, R., 2003. Climate change and urban stormwater infrastructure in Canada: Context and case studies. Toronto-Niagara Region Study Report and Working Paper Series Rep. No. 2003-1, Meteorological Service of Canada, Waterloo, Ontario.

Willems, P., Arnbjerg-Nielsen, K., Olsson, J. and Nguyen, V. T. V., 2012. Climate change impact assessment on urban rainfall extremes and urban drainage: Methods and shortcomings. Atmospheric research, 103, pp.106-118.

Zhang, Y., Zhang, Z., Reed, S., and Koren, V., 2011. An enhanced and automated approach for deriving a priori SAC-SMA parameters from the soil survey geographic database. Computers and Geosciences, 37(2), 219231.

List of figure captions

Fig 1. Schematic of the one-way coupling of the storm drain module and the natural channel routing module of RDHM.

Fig 2a. Actual storm drain network for the five urban catchments overlaid on a 250 m grid.

Fig 2b. Same as Fig 2a but for the equivalent storm drain network.

Fig 3. Five urban catchments in the Cities of Arlington and Grand Prairie used in the integrated modeling.

Fig 4. Comparison at selected outfall locations of flow hydrographs from the actual and equivalent storm drain systems.

Fig 5. Comparison of the inlet flow-vs.-water depth relationship from four different weir and orifice equations for three different inlet lengths.

Fig 6a. Observed vs. simulated streamflow with and without SDM at GP6363 for the November 2015 event. The rainfall forcing used is the CASA QPE.

Fig 6b. Same as Fig 6a but for the December 2015 event.

Fig 6c. Comparison at selected locations of observed water level vs. simulated flow with and without SDM for the January 16, 2017, event.

Fig 7. Simulated hydrographs of channel flow with and without SDM at all grid boxes for the Johnson Creek Catchment (Outlet GP6033) due to 100-yr 5-min rainfall.

Fig 8. Same as Fig 7 but box-and-whisker plot representation the hydrographs in logarithmic scale.

Fig 9. Ratio of the simulated flow with SDM to that without at each grid box in the Johnson Creek Catchment (Outlet 6033) due to 100-yr 5-min rainfall.

Fig 10a. Box-and-whisker plots of the hydrographs in logarithmic scale at all grid boxes with and without SDM for the Johnson Creek Catchment (Outlet GP6033) for the January 16, 2017, event.

Fig 10b. Same as Fig 10a but for the May 29, 2015, event.

Fig 11. Map of the peak flow ratio (PFR), i.e., the ratio of the peak flow with SDM to that without for 100-yr 24-hr rainfall for the entire study area.

Fig 12. Same as Fig 11 but only for those cells that do not contain outfalls and with PFR > 1.

Fig 13. Same as Fig 11 but under a uniform 15% increase in imperviousness in all catchments.

Fig 14. Volume of stormwater conveyed by natural channels (solid line) vs. storm drains (dashed line) for five different inlet lengths due to spatially-uniform 100-yr 5-min rainfall. The total volume (dotted black line) is the same as the sum of the two volumes represented by solid and dashed lines of a same color for each inlet length.

Fig 1

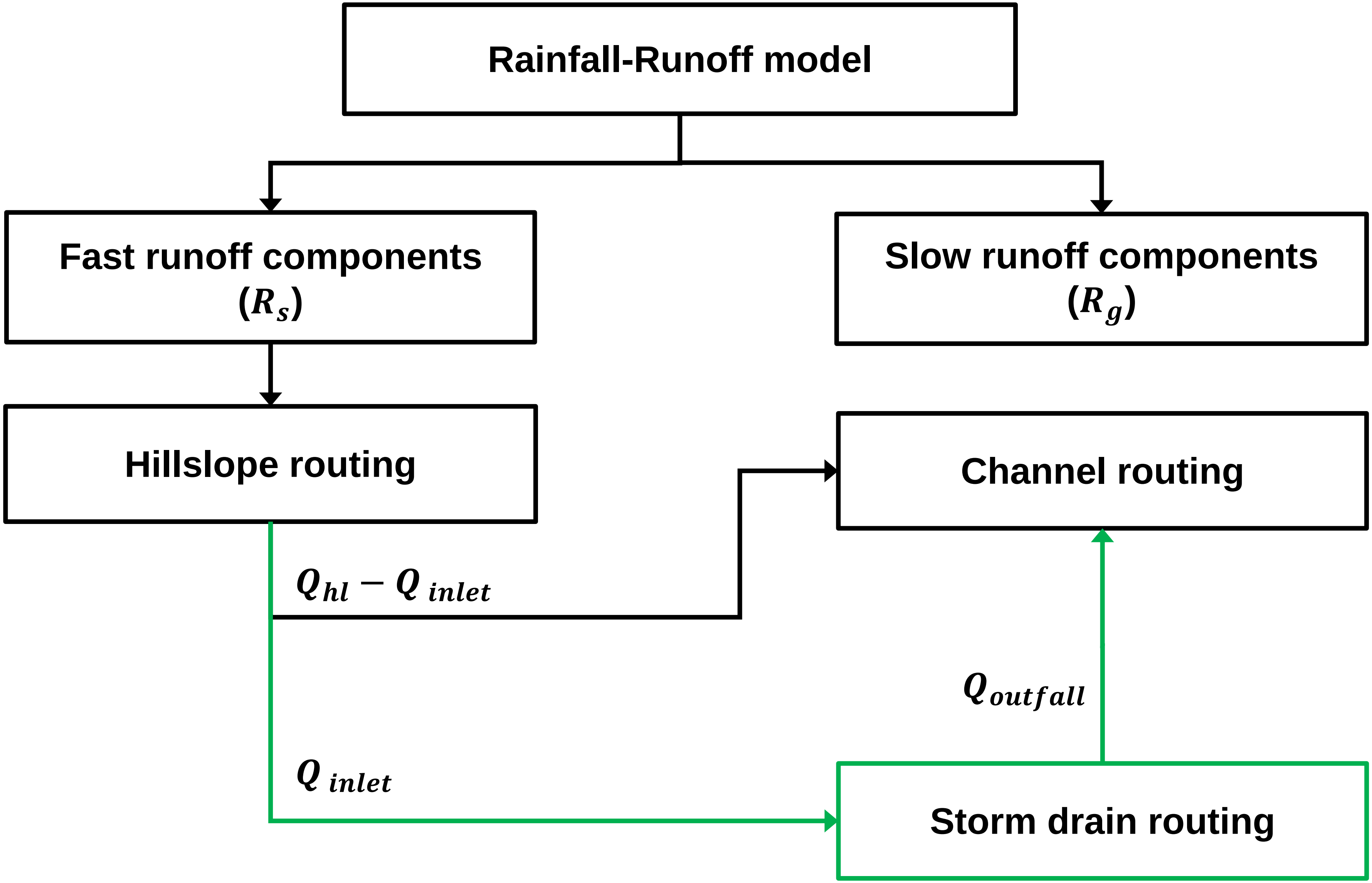

Rainfall-Runoff model
Fast runoff components
(R_s)
Slow runoff components
(R_g)
Hillslope routing
Channel routing
$Q_{hl} - Q_{inlet}$
$Q_{outfall}$
Q_{inlet}
Storm drain routing

Fig 2a

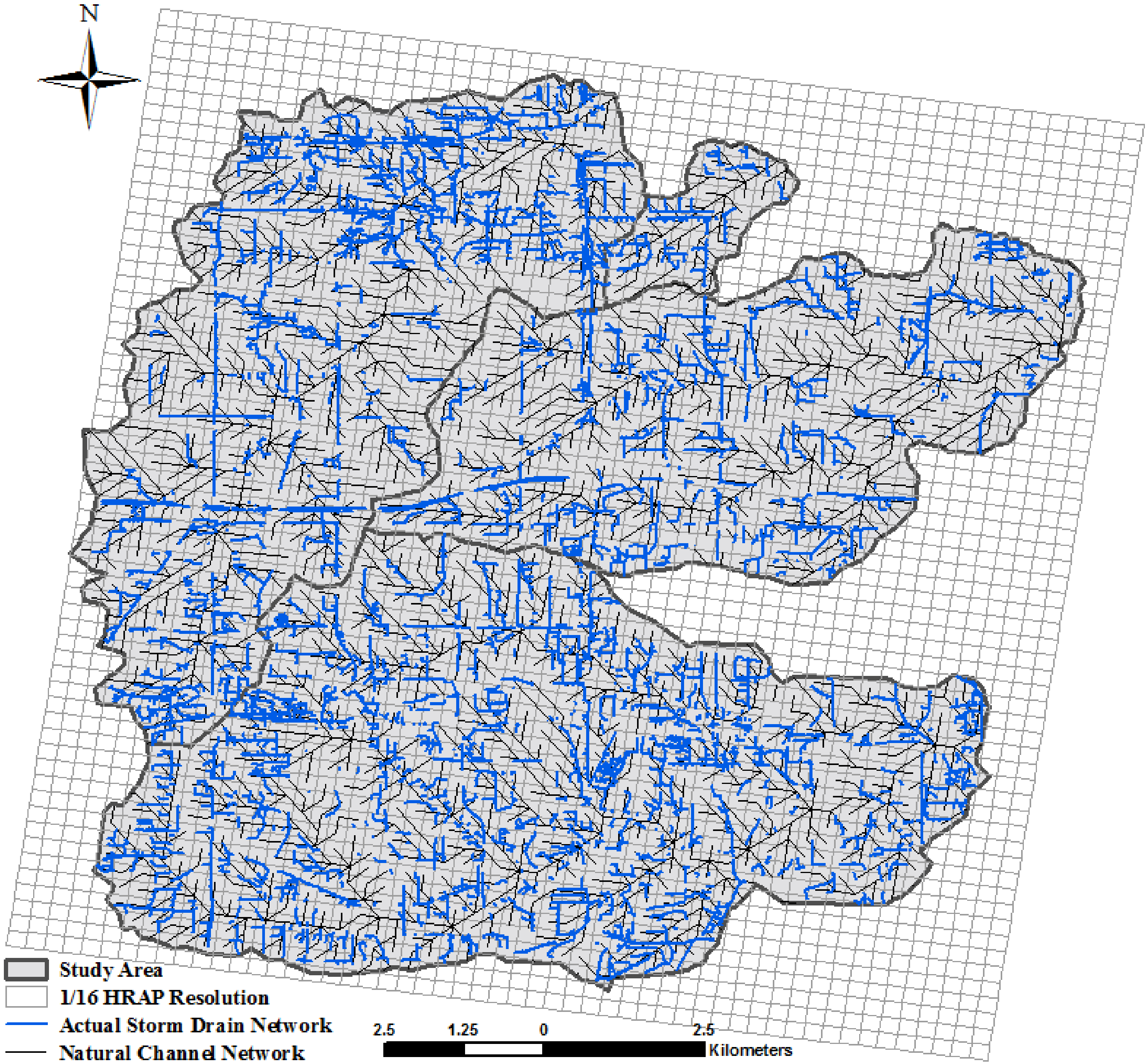
N
Study Area
1/16 HRAP Resolution
Actual Storm Drain Network
Natural Channel Network
2.5
1.25
0
2.5
Kilometers

Fig 2b

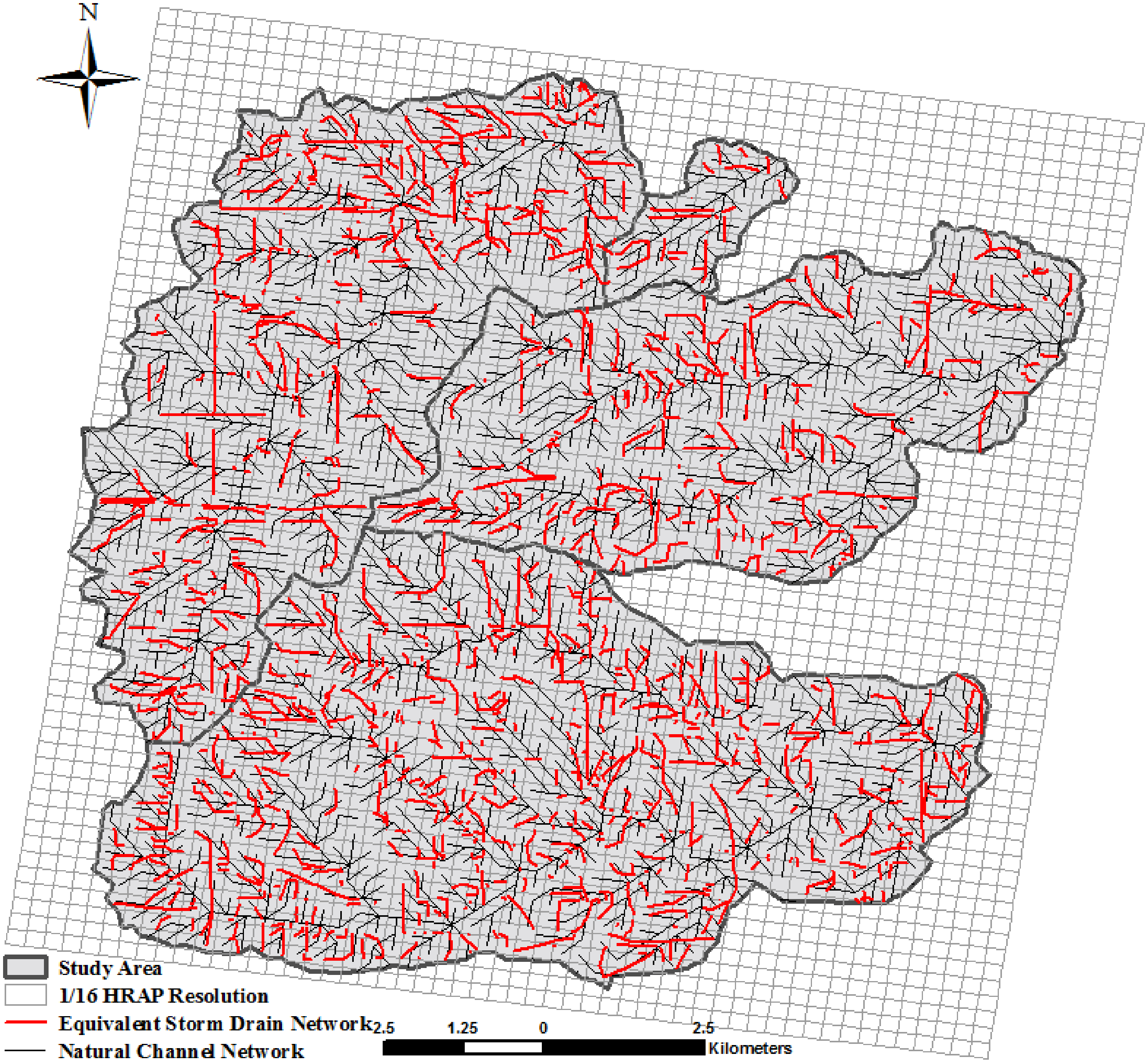

N
Study Area
1/16 HRAP Resolution
Equivalent Storm Drain Network
Natural Channel Network
2.5
1.25
0
2.5
Kilometers

Fig 3

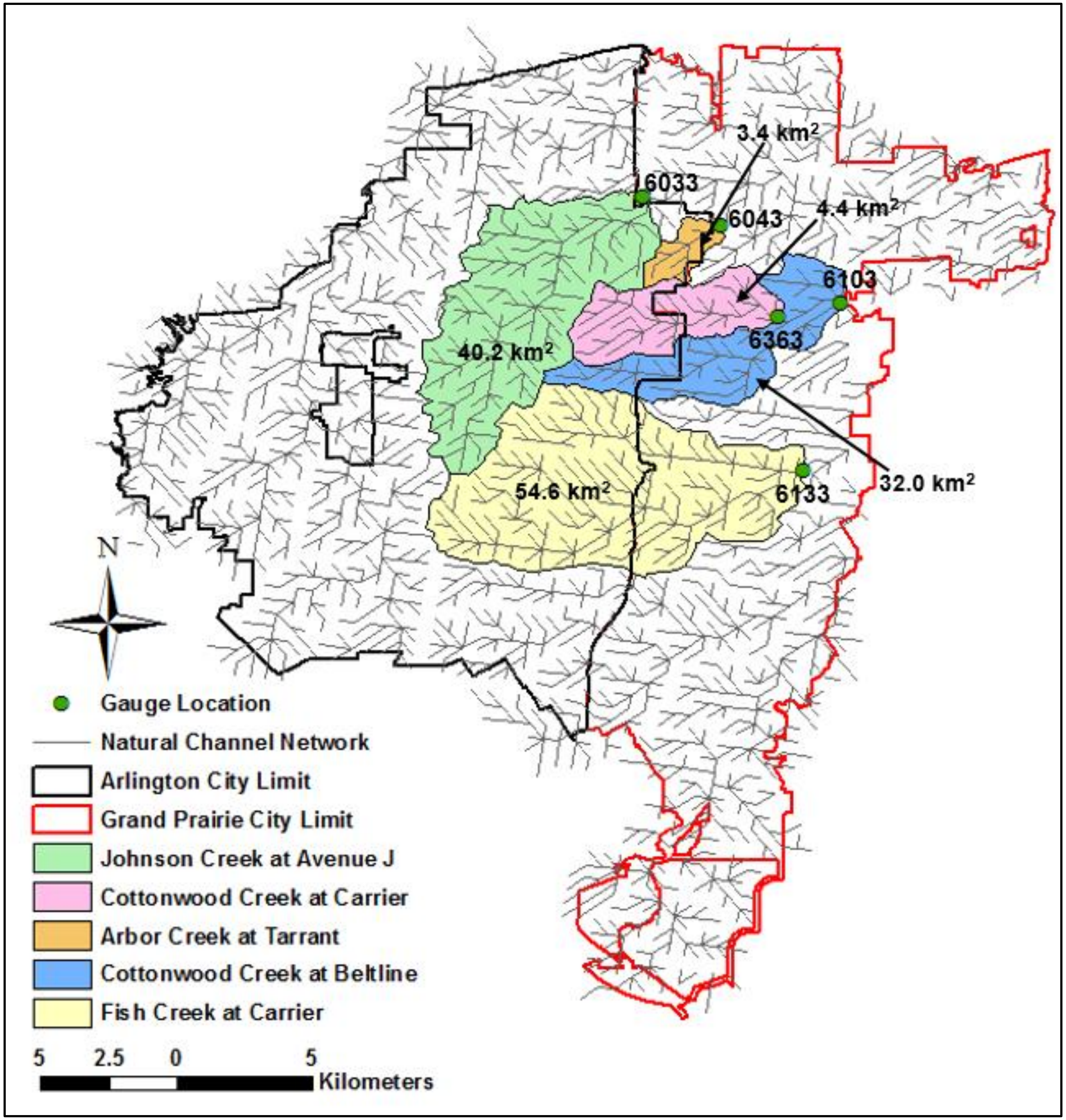
3.4 km²
6033
6043
4.4 km²
6103
6363
40.2 km²
32.0 km²
54.6 km²
6133
N
Gauge Location
Natural Channel Network
Arlington City Limit
Grand Prairie City Limit
Johnson Creek at Avenue J
Cottonwood Creek at Carrier
Arbor Creek at Tarrant
Cottonwood Creek at Beltline
Fish Creek at Carrier
5 2.5 0 5
Kilometers

Fig 4

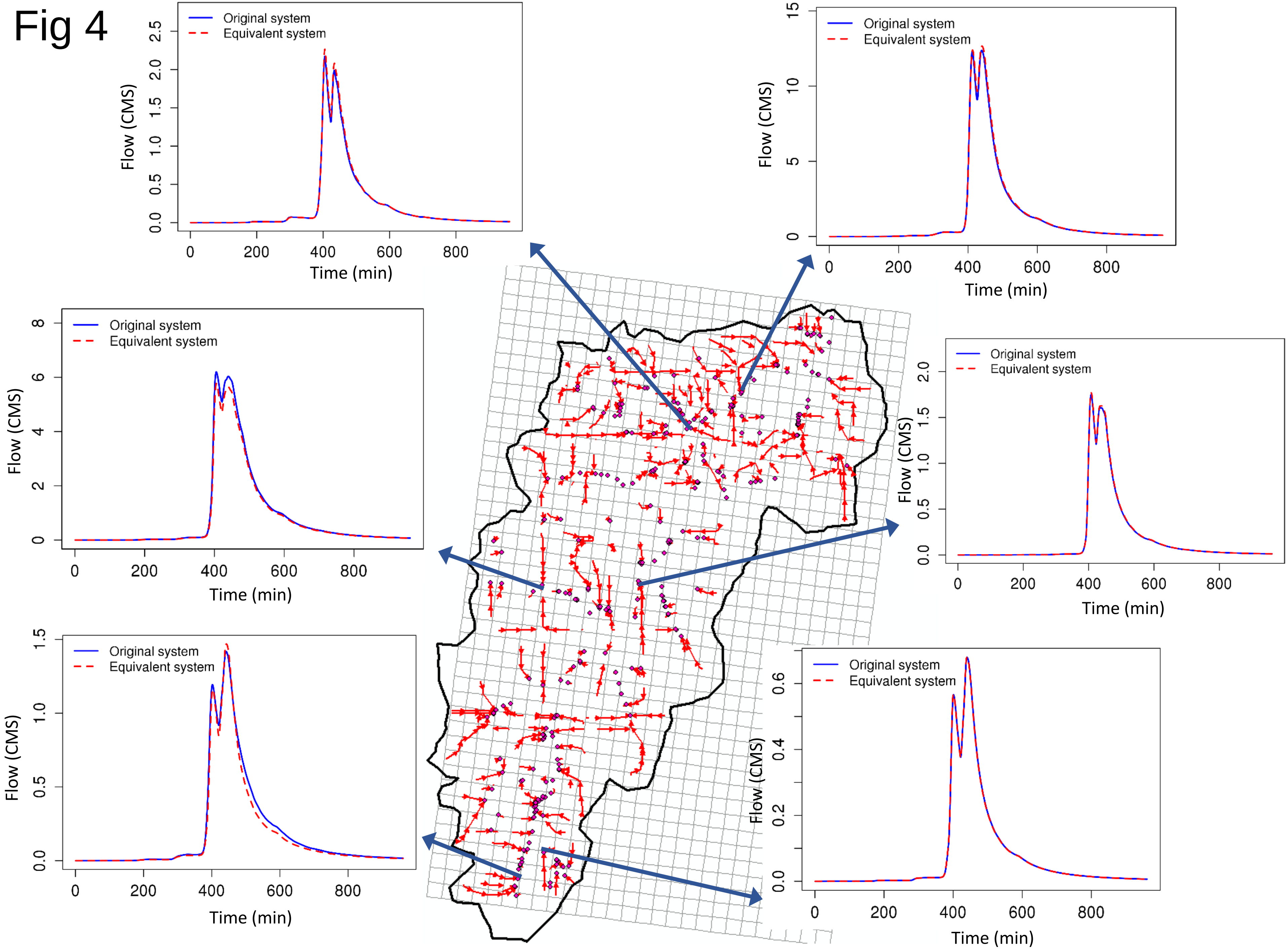

Original system
Equivalent system
Flow (CMS)
0.0 0.5 1.0 1.5 2.0 2.5
0 200 400 600 800
Time (min)
Original system
Equivalent system
Flow (CMS)
0 5 10 15
0 200 400 600 800
Time (min)
Original system
Equivalent system
Flow (CMS)
0 2 4 6 8
0 200 400 600 800
Time (min)
Original system
Equivalent system
Flow (CMS)
0.0 0.5 1.0 1.5 2.0
0 200 400 600 800
Time (min)
Original system
Equivalent system
Flow (CMS)
0.0 0.5 1.0 1.5
0 200 400 600 800
Time (min)
Original system
Equivalent system
Flow (CMS)
0.0 0.2 0.4 0.6
0 200 400 600 800
Time (min)

Fig 5

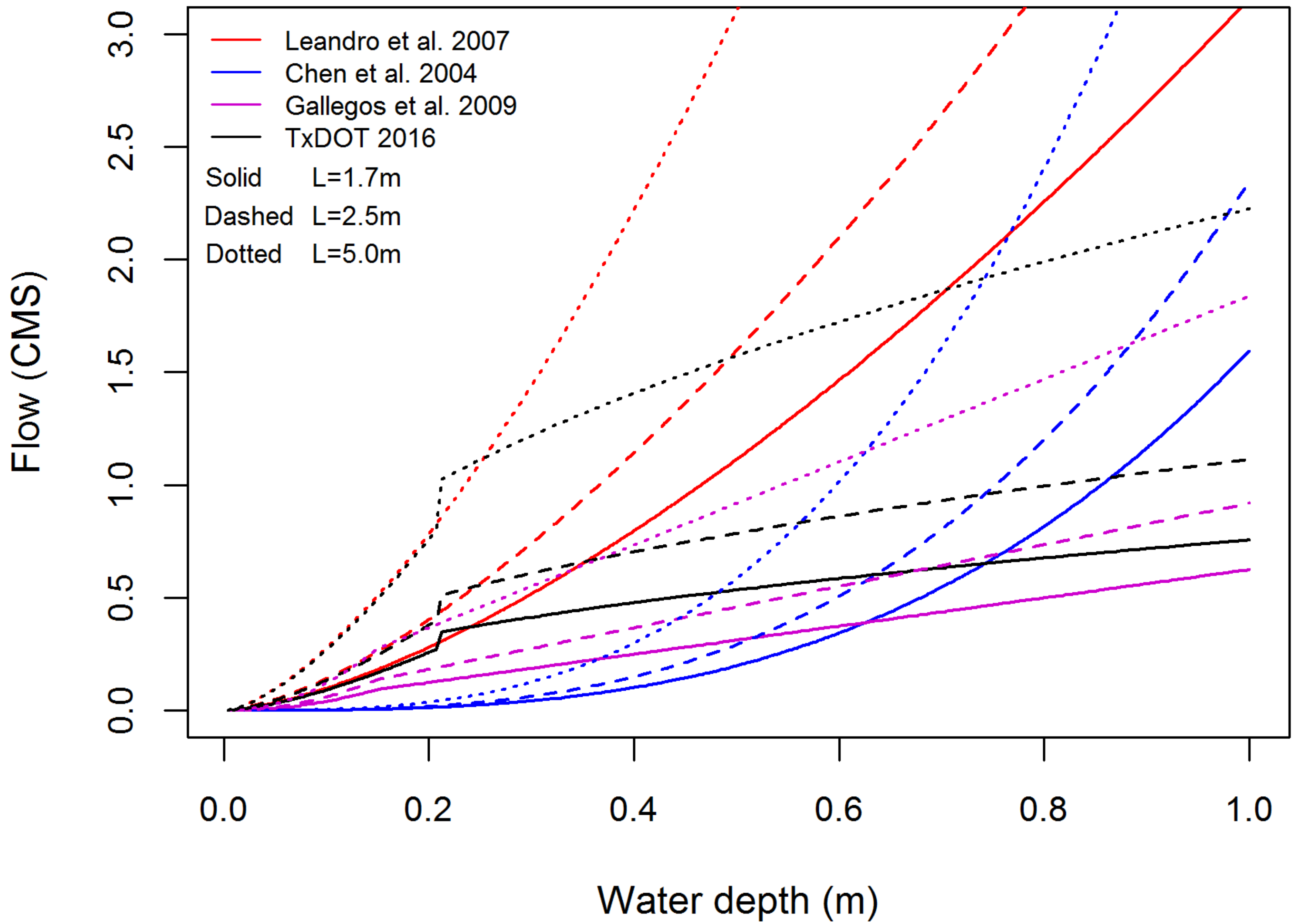
Leandro et al. 2007
Chen et al. 2004
Gallegos et al. 2009
TxDOT 2016
Solid L=1.7m
Dashed L=2.5m
Dotted L=5.0m
Flow (CMS)
Water depth (m)
0.0
0.5
1.0
1.5
2.0
2.5
3.0
0.0
0.2
0.4
0.6
0.8
1.0

Fig 6a

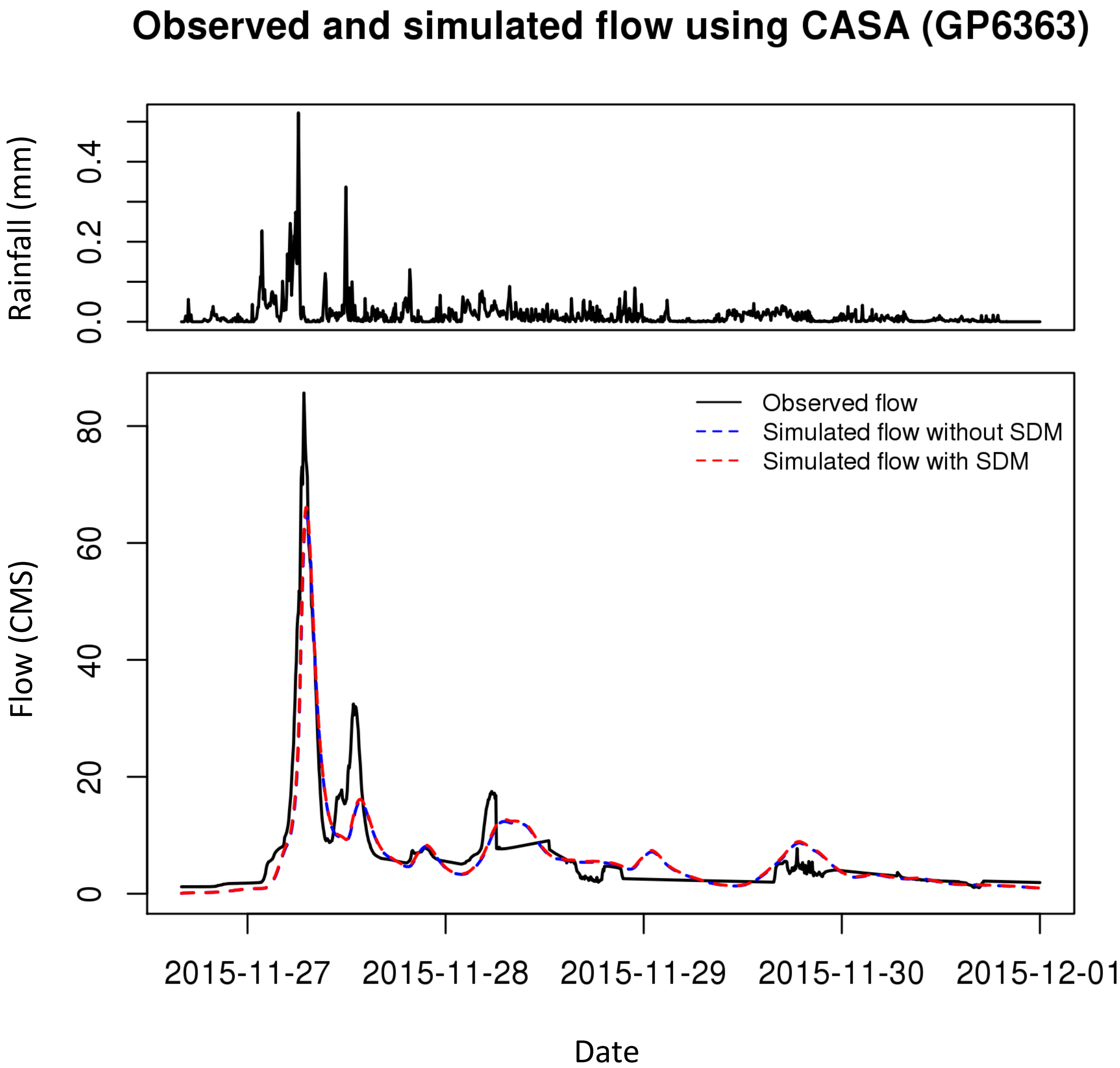
Observed and simulated flow using CASA (GP6363)
Rainfall (mm)
0.0
0.2
0.4
Flow (CMS)
0
20
40
60
80
Observed flow
Simulated flow without SDM
Simulated flow with SDM
2015-11-27
2015-11-28
2015-11-29
2015-11-30
2015-12-01
Date

Fig 6b

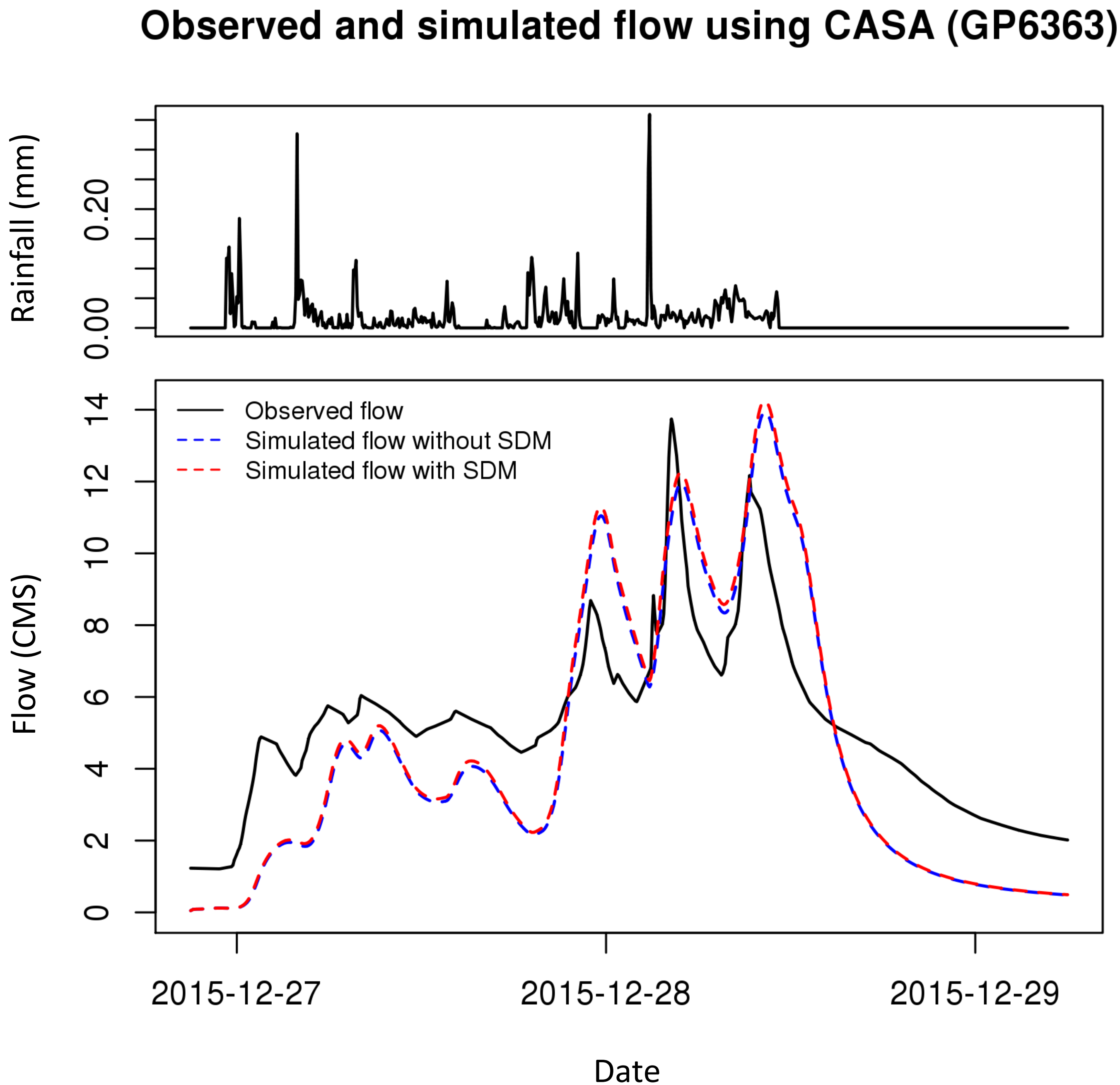

Observed and simulated flow using CASA (GP6363)
Rainfall (mm)
0.00
0.20
Flow (CMS)
0
2
4
6
8
10
12
14
Observed flow
Simulated flow without SDM
Simulated flow with SDM
2015-12-27
2015-12-28
2015-12-29
Date

Fig 6c

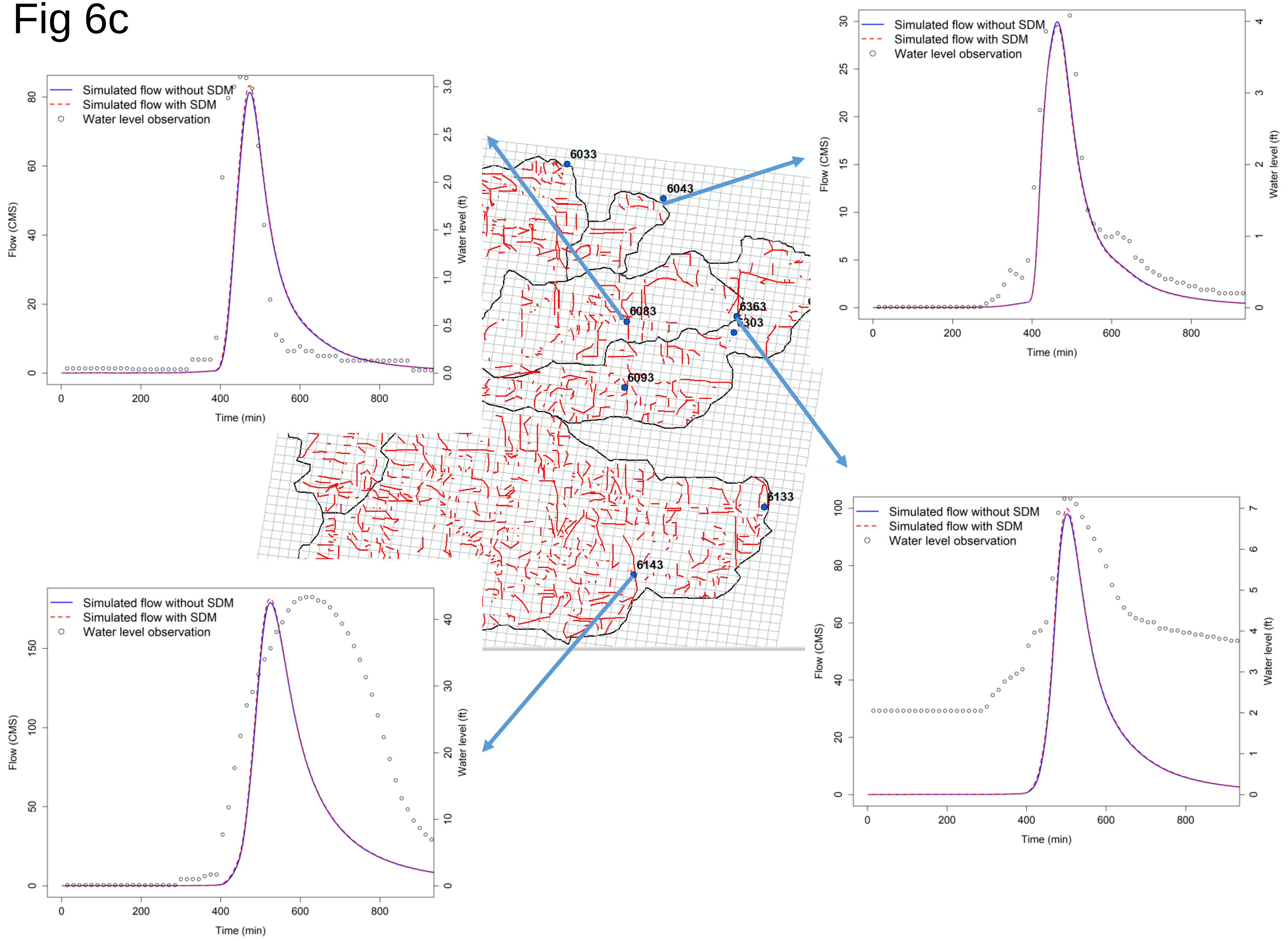

Simulated flow without SDM
Simulated flow with SDM
Water level observation
Flow (CMS)
Water level (ft)
Time (min)
6033
6043
6083
6363
6093
6133
6143

Fig 7

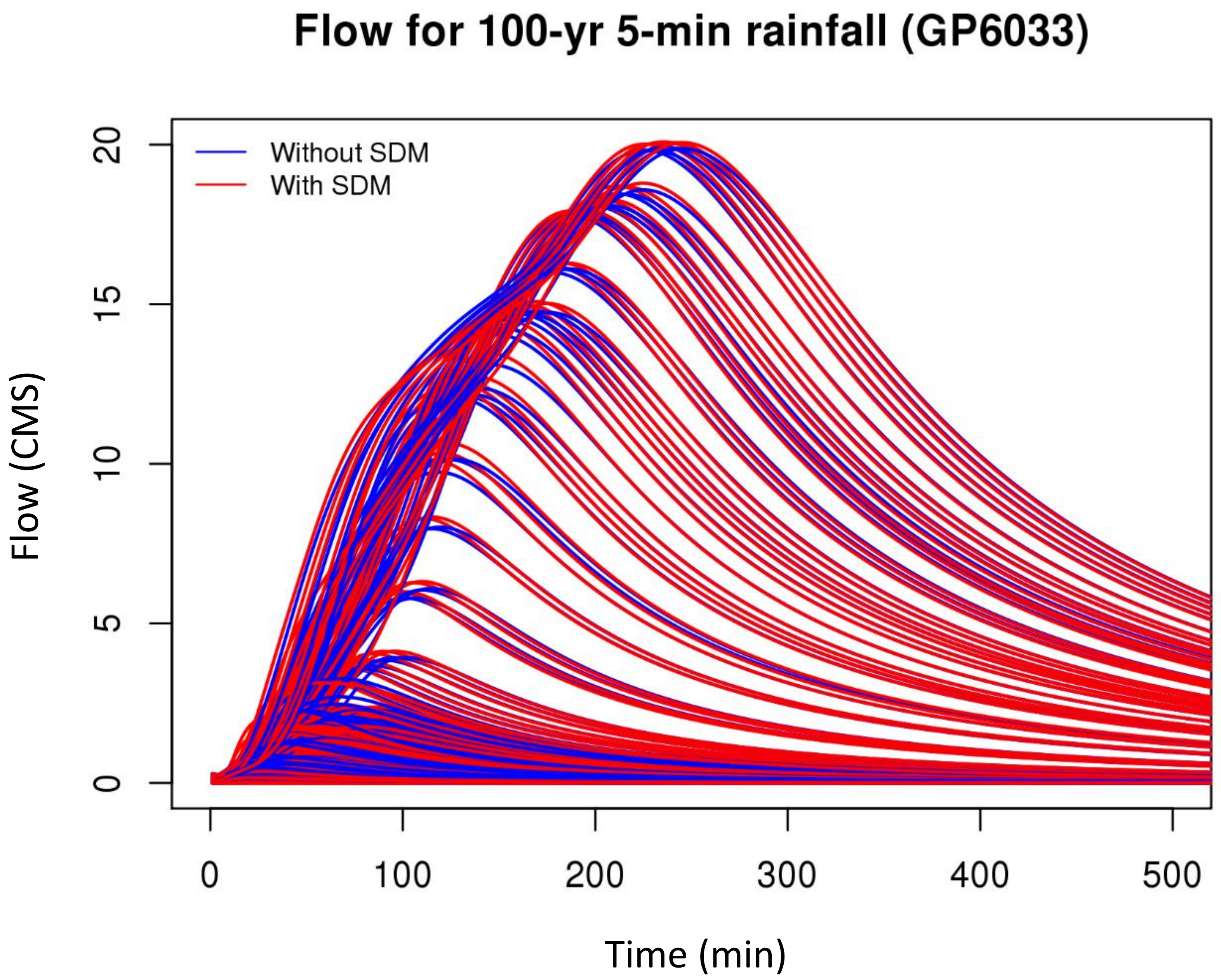

Flow for 100-yr 5-min rainfall (GP6033)
Without SDM
With SDM
Flow (CMS)
0
5
10
15
20
0
100
200
300
400
500
Time (min)

Fig 8

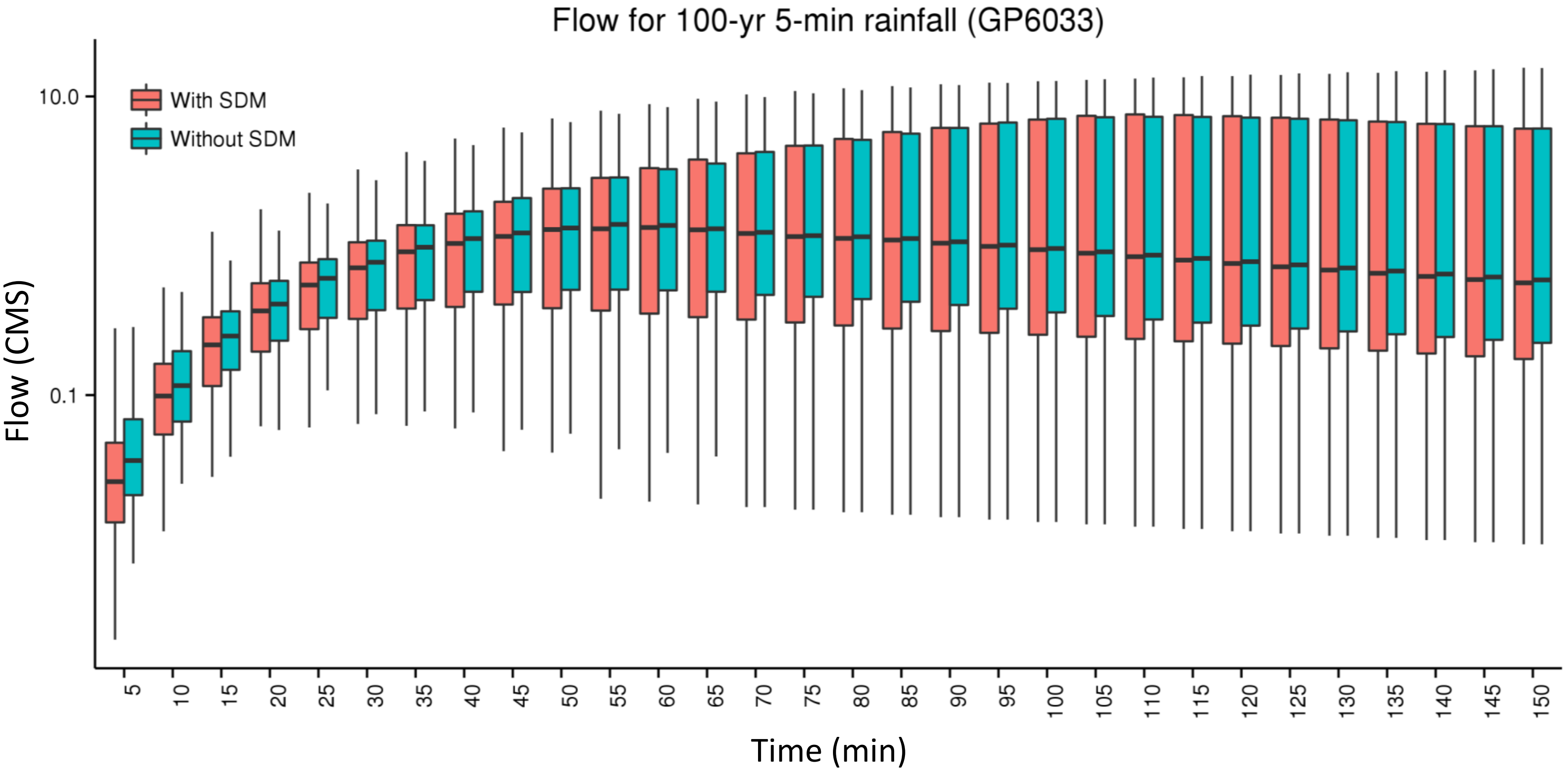

Flow for 100-yr 5-min rainfall (GP6033)
With SDM
Without SDM
10.0
0.1
Flow (CMS)
5
10
15
20
25
30
35
40
45
50
55
60
65
70
75
80
85
90
95
100
105
110
115
120
125
130
135
140
145
150
Time (min)

Fig 9

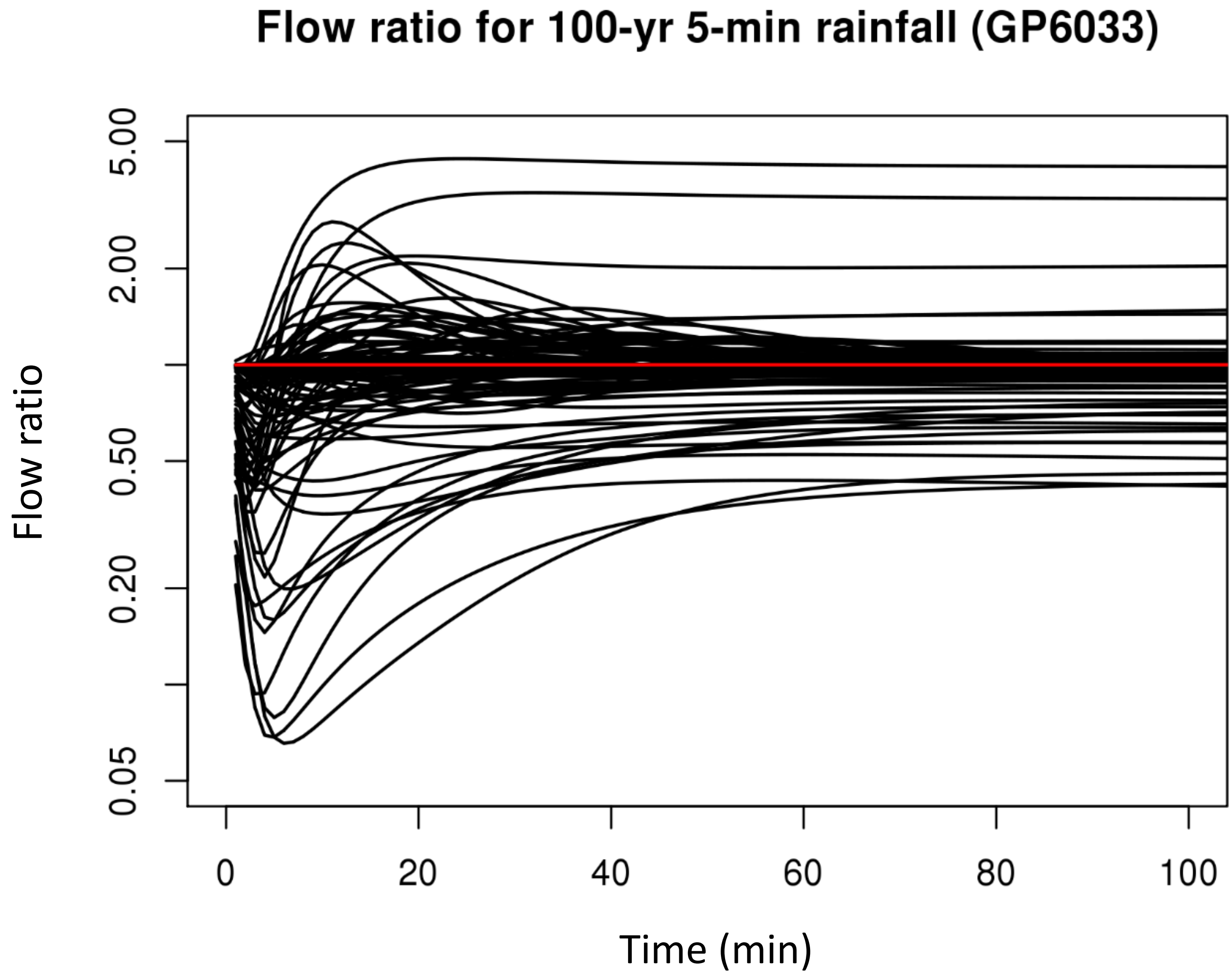
Flow ratio for 100-yr 5-min rainfall (GP6033)
Flow ratio
5.00
2.00
0.50
0.20
0.05
0
20
40
60
80
100
Time (min)

Fig 10a

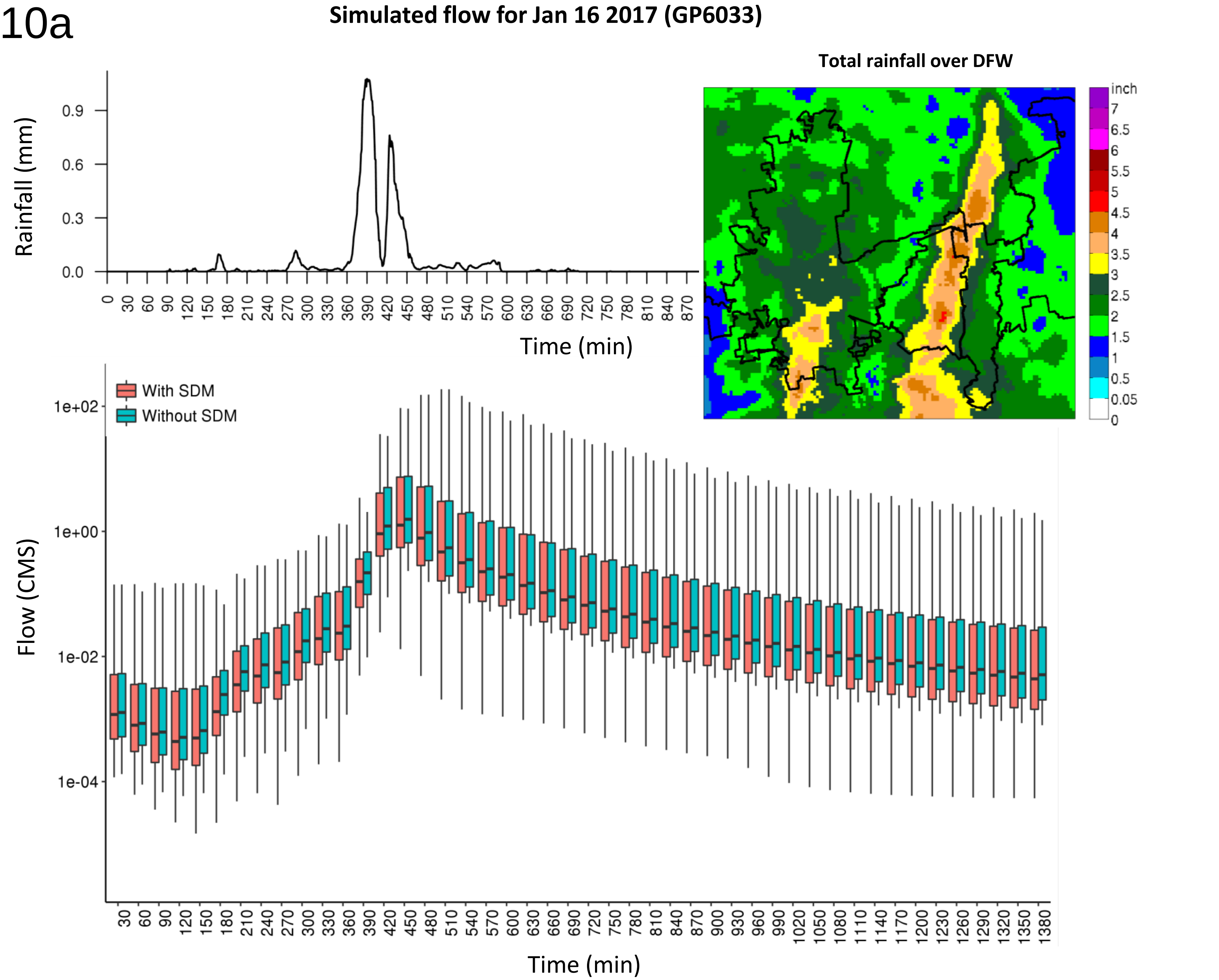
Simulated flow for Jan 16 2017 (GP6033)
Rainfall (mm)
0.9
0.6
0.3
0.0
Time (min)
0 30 60 90 120 150 180 210 240 270 300 330 360 390 420 450 480 510 540 570 600 630 660 690 720 750 780 810 840 870
Total rainfall over DFW
inch
7 6.5 6 5.5 5 4.5 4 3.5 3 2.5 2 1.5 1 0.5 0.05 0
Flow (CMS)
With SDM
Without SDM
1e+02
1e+00
1e-02
1e-04
Time (min)
30 60 90 120 150 180 210 240 270 300 330 360 390 420 450 480 510 540 570 600 630 660 690 720 750 780 810 840 870 900 930 960 990 1020 1050 1080 1110 1140 1170 1200 1230 1260 1290 1320 1350 1380

Fig 10b

Simulated flow for May 29 2015 (GP6033)

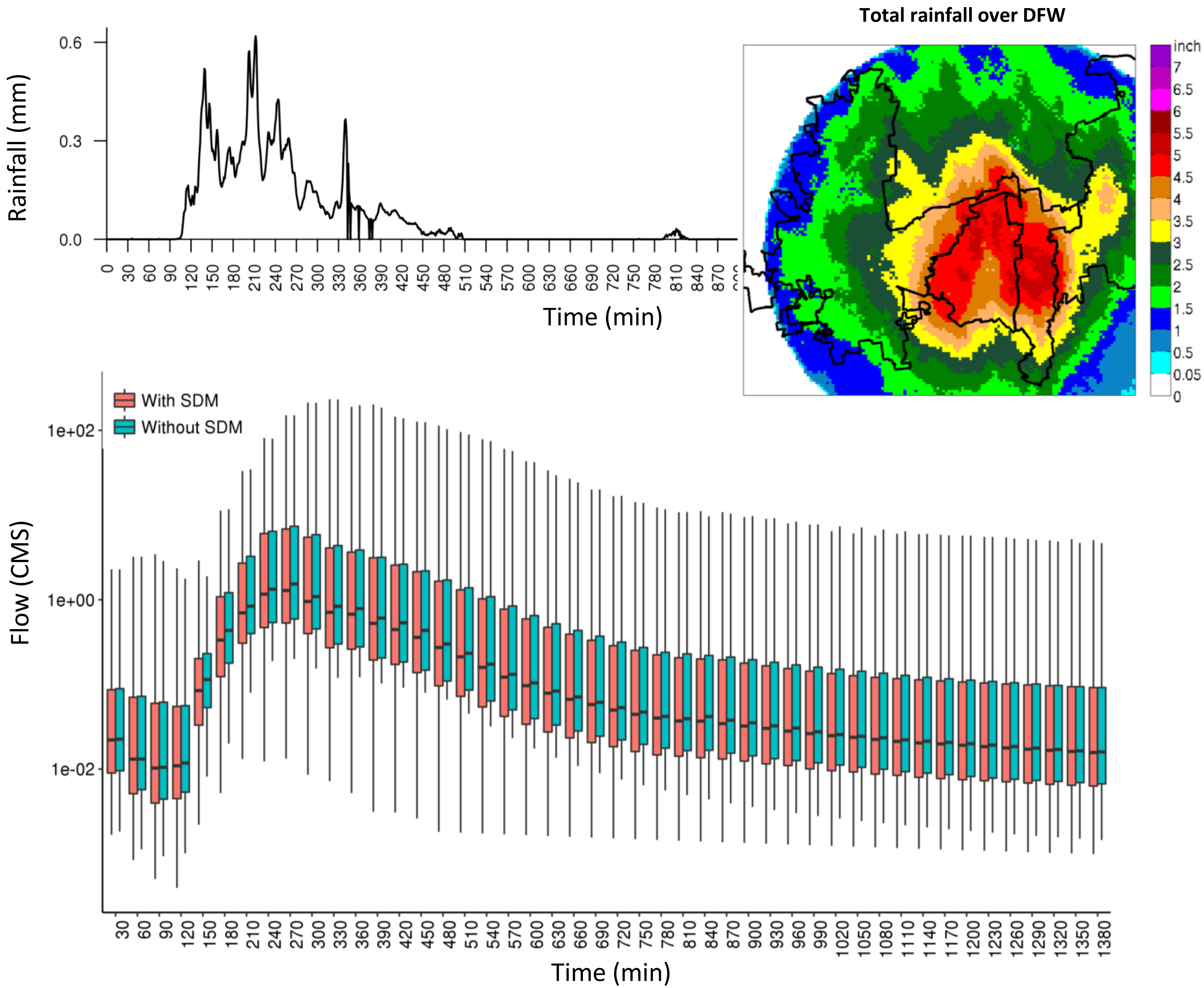

Fig 11

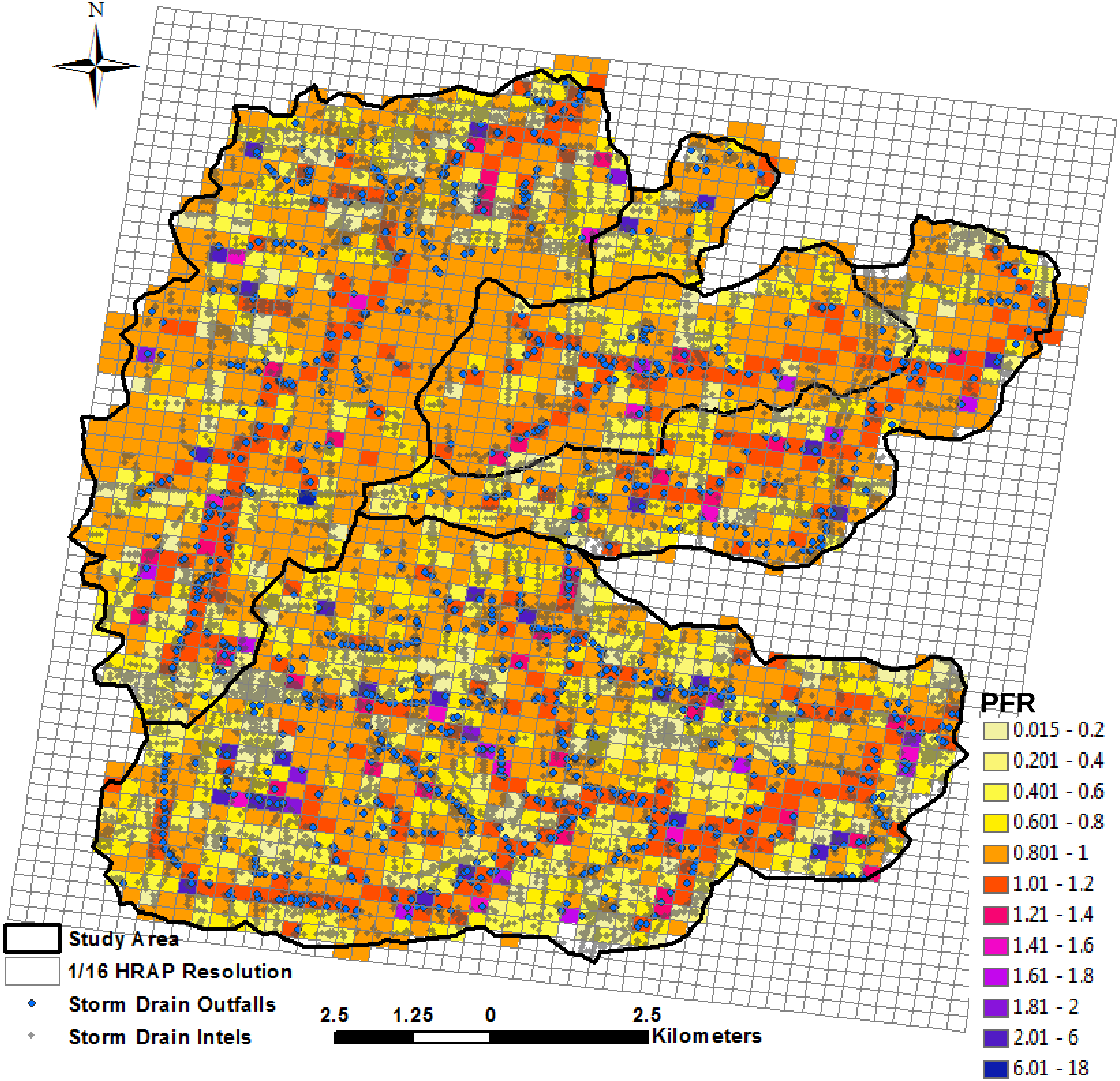
N
PFR
0.015 - 0.2
0.201 - 0.4
0.401 - 0.6
0.601 - 0.8
0.801 - 1
1.01 - 1.2
1.21 - 1.4
1.41 - 1.6
1.61 - 1.8
1.81 - 2
2.01 - 6
6.01 - 18
Study Area
1/16 HRAP Resolution
Storm Drain Outfalls
Storm Drain Intels
2.5 1.25 0 2.5
Kilometers

Fig 12

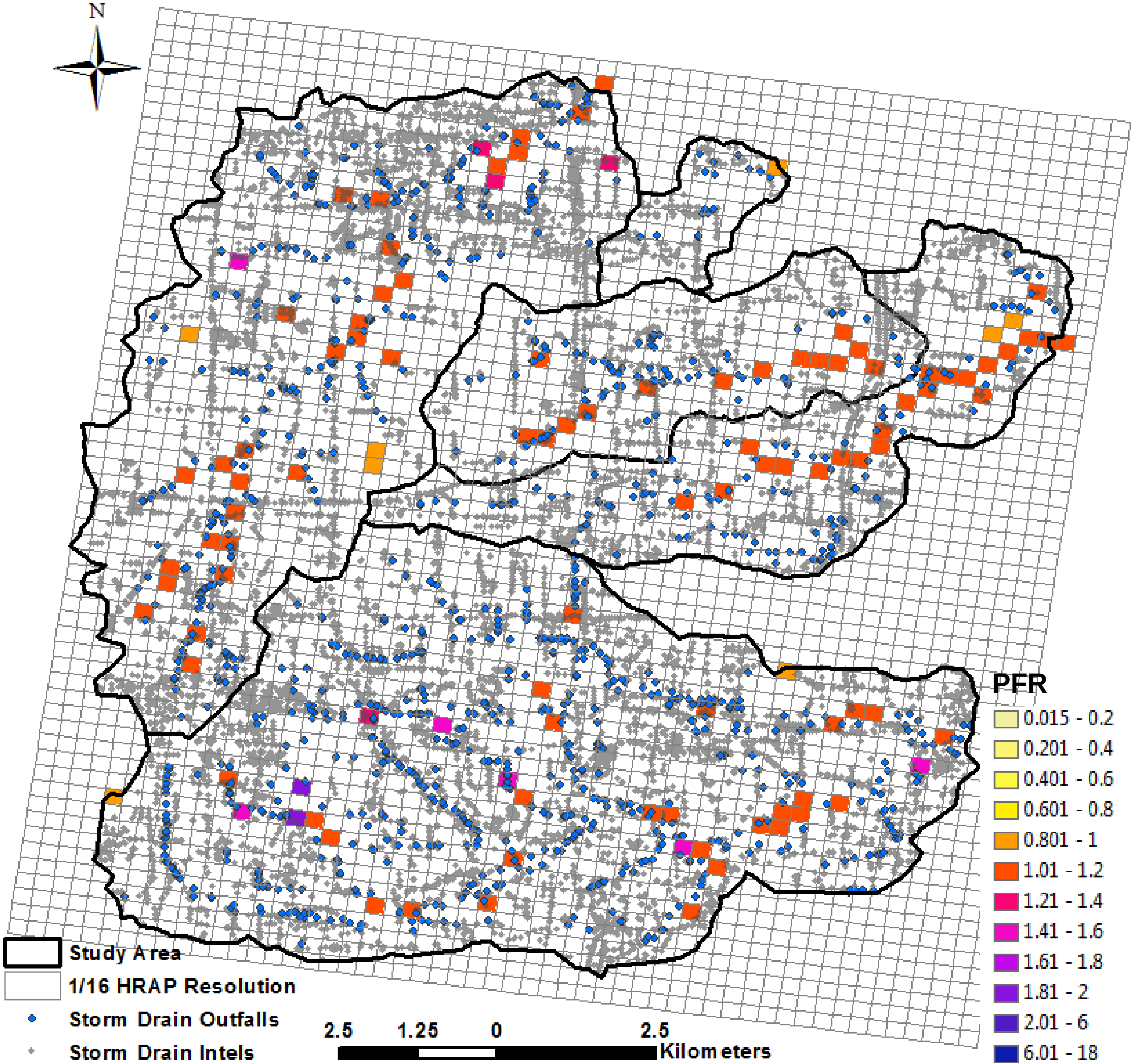
N
PFR
0.015 - 0.2
0.201 - 0.4
0.401 - 0.6
0.601 - 0.8
0.801 - 1
1.01 - 1.2
1.21 - 1.4
1.41 - 1.6
1.61 - 1.8
1.81 - 2
2.01 - 6
6.01 - 18
Study Area
1/16 HRAP Resolution
Storm Drain Outfalls
Storm Drain Intels
2.5 1.25 0 2.5
Kilometers

Fig 13

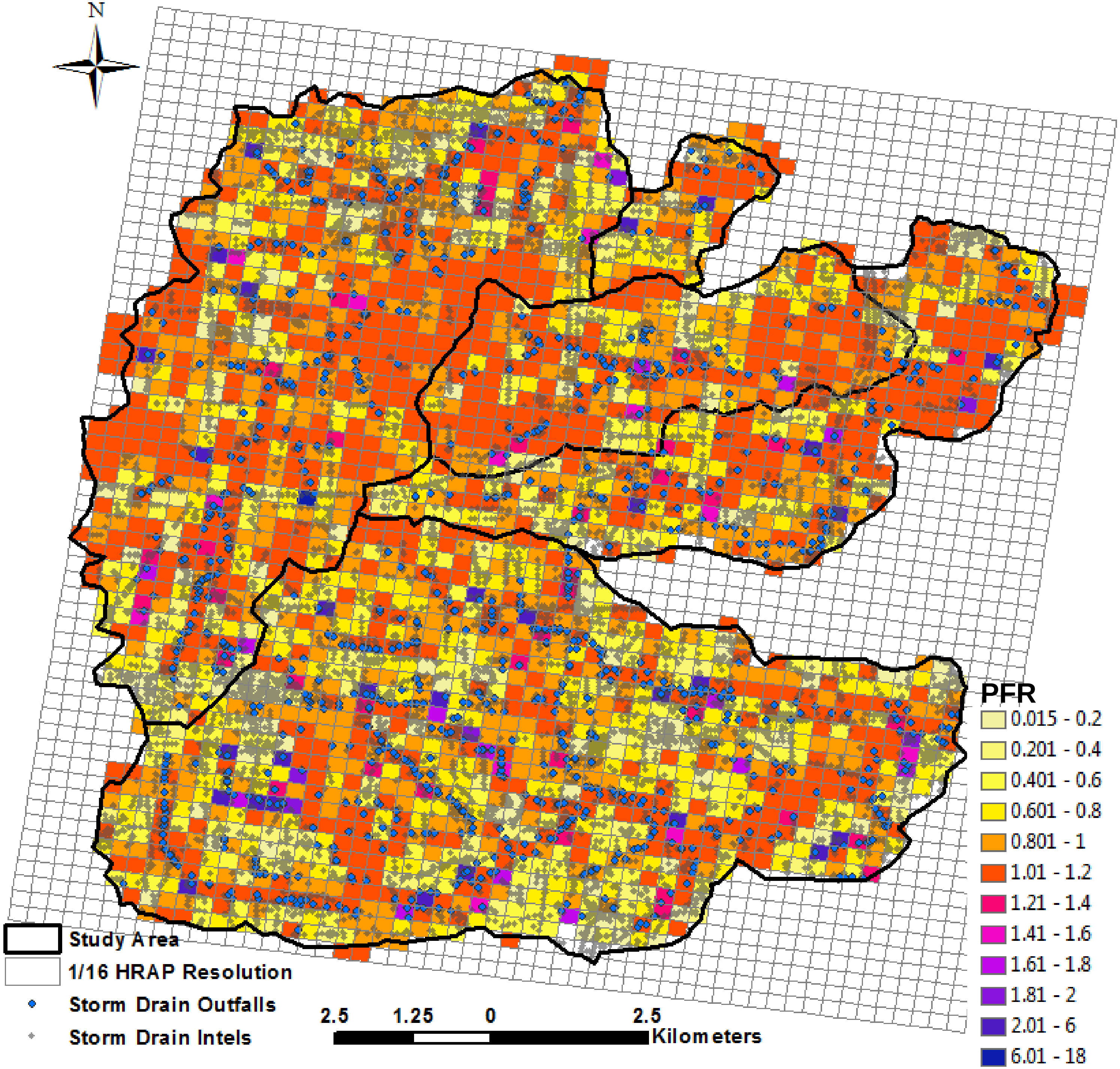
N
PFR
0.015 - 0.2
0.201 - 0.4
0.401 - 0.6
0.601 - 0.8
0.801 - 1
1.01 - 1.2
1.21 - 1.4
1.41 - 1.6
1.61 - 1.8
1.81 - 2
2.01 - 6
6.01 - 18
Study Area
1/16 HRAP Resolution
Storm Drain Outfalls
Storm Drain Intels
2.5 1.25 0 2.5
Kilometers

Fig 14

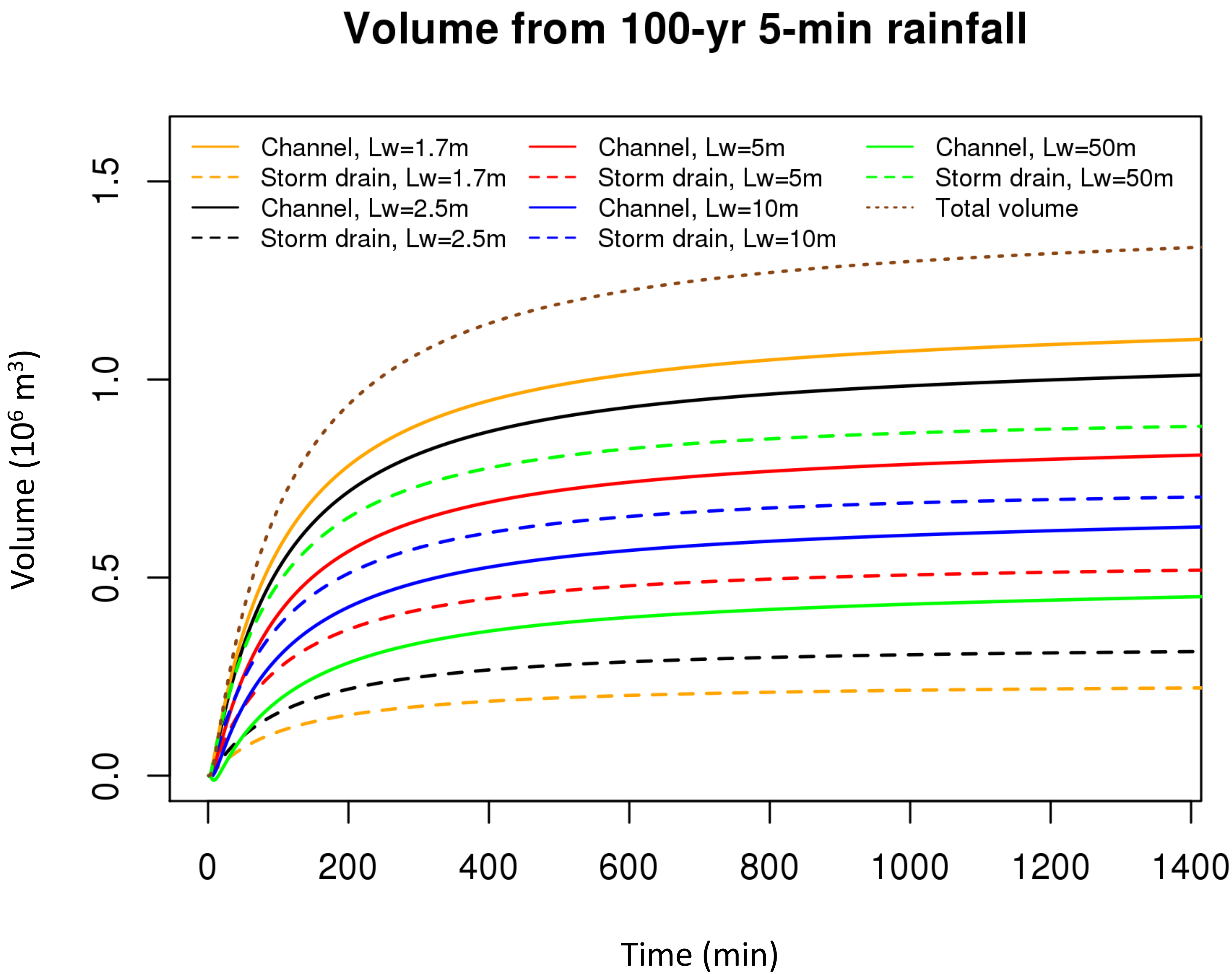
Volume from 100-yr 5-min rainfall
Channel, Lw=1.7m
Storm drain, Lw=1.7m
Channel, Lw=2.5m
Storm drain, Lw=2.5m
Channel, Lw=5m
Storm drain, Lw=5m
Channel, Lw=10m
Storm drain, Lw=10m
Channel, Lw=50m
Storm drain, Lw=50m
Total volume
Volume (10^6 m^3)
0.0
0.5
1.0
1.5
0
200
400
600
800
1000
1200
1400
Time (min)